MARSHALL, DANIEL RAY

A MICHELSON INTERFEROMETER OBJECTIVE FOR SURFACE PROFILING.

THE UNIVERSITY OF ARIZONA M.S. 1984

PLEASE NOTE:

In all cases this material has been filmed in the best possible way from the available copy. Problems encountered with this document have been identified here with a check mark _√_.

1. Glossy photographs or pages _____
2. Colored illustrations, paper or print _____
3. Photographs with dark background _____
4. Illustrations are poor copy _____
5. Pages with black marks, not original copy _____
6. Print shows through as there is text on both sides of page _____
7. Indistinct, broken or small print on several pages ✓
8. Print exceeds margin requirements _____
9. Tightly bound copy with print lost in spine _____
10. Computer printout pages with indistinct print _____
11. Page(s) _____ lacking when material received, and not available from school or author.
12. Page(s) _____ seem to be missing in numbering only as text follows.
13. Two pages numbered _____. Text follows.
14. Curling and wrinkled pages _____
15. Other _____

A MICHELSON INTERFEROMETER OBJECTIVE FOR SURFACE PROFILING

by

Daniel Ray Marshall

A Thesis Submitted to the Faculty of the

COMMITTEE ON OPTICAL SCIENCES (GRADUATE)

In Partial Fulfillment of the Requirements

For the Degree of

MASTER OF SCIENCE

In the Graduate College

THE UNIVERSITY OF ARIZONA

1 9 8 4

STATEMENT BY AUTHOR

This thesis has been submitted in partial fulfillment of requirements for an advanced degree at The University of Arizona and is deposited in the University Library to be made available to borrowers under rules of the Library.

Brief quotations from this thesis are allowable without special permission, provided that accurate acknowledgment of source is made. Requests for permission for extended quotation from or reproduction of this manuscript in whole or in part may be granted by the head of the major department or the Dean of the Graduate College when in his or her judgment the proposed use of the material is in the interests of scholarship. In all other instances, however, permission must be obtained from the author.

SIGNED: Daniel Ray Marshall

APPROVAL BY THESIS DIRECTOR

This thesis has been approved on the date shown below:

James C. Wyant
Professor of Optical Sciences

July 12, 1989
Date

ACKNOWLEDGMENTS

I would like to thank my advisor, James C. Wyant, for his accessibility and for his many constructive suggestions which have been incorporated into this thesis project. I would also like to thank Roland Shack for his generous gift of time and insight, not only relating to this project, but throughout the past two years.

In preparing this document I was fortunate to have the assistance of Lisa DuBois (typing) and Jim Osgood (illustrations) to carry me through the anxious process of polishing the final product.

To Wyko Optical, Inc. I owe a debt of gratitude for supporting the research on which this thesis is based. Likewise I am indebted to many students, members of the faculty and staff of the Optical Sciences Center of the University of Arizona for enlightment, inspiration and assistance.

And finally I wish to thank my wife Barbara and my son Brian for their patience, enthusiasm and understanding through the past two years.

TABLE OF CONTENTS

LIST OF ILLUSTRATIONS

LIST OF ILLUSTRATIONS—Continued

ABSTRACT

The design of a Michelson interferometer for use with an existing interferometric surface profiler is described.

Choice of interferometer type is described based on a review of two-beam interferometry and unsuitability of the existing Mirau interferometer at low magnification because of obscuration problems. A Michelson configuration is chosen which places a cube beamsplitter between the microscope objective and the test surface.

A number of parameters, including geometrical and physical optics and mechanical performance criteria, are used to aid modeling and decision making in an explicitly described design process. The critical component is found to be the beamsplitter, and criteria are developed for characterizing and selecting cube beamsplitters for use in this application.

The configurations of three alternative versions of the device are discussed. Assembly drawings are included. Testing of the finished device is described, and while the completed interferometer is found to be usable, recommendations are made for improvement of the performance through installation of a better beamsplitter and use of an alternative method of illumination.

CHAPTER 1

INTRODUCTION

An existing commercial interferometric instrument (NCP-1000 Optical Profiler manufactured by Wyko Optical Co., Tucson, Arizona) has the capability of measuring surface profiles of suitable samples with a resolution of better than 1/1000 of a wavelength of visible light (Koliopoulos, 1981). The instrument uses a Mirau interferometric objective to investigate a well-defined range of spatial frequencies using sophisticated optoelectronic and digital techniques. This thesis describes the design and testing of an interferometric objective of the Michelson type which can be used with the existing profiler in place of the Mirau objective to investigate lower spatial frequencies than are accessible with the Mirau type.

This project required the development of an optomechanical device which would meet a list of fairly stringent, yet open-ended requirements. The result was a classical design project in which it was necessary to generate a design program, sketch some physical forms which would satisfy the requirements, select the best features from each concept, and then iteratively refine the basic idea until it was satisfactory.

The following discussion reflects the design process, although rather imperfectly. It is representative to the extent that it touches upon all of the steps which were involved in the process. It is

imperfect to the extent that the reader may be left with the impressions (1) that this is the only solution to the problem; and (2) that the development was linear and direct. This is far from the case! Any solution is, of course, only one set of compromises (some of them subtle and rather convoluted) which satisfies the design requirements; and even more importantly, it came about through many repetitions of the basic formula: define, explore, develop and test (see Figure 1).

This thesis will discuss the design goals which shaped the evolution of the interferometric objective, describe the detailed design development, and summarize the performance of the finished instrument.

Design Goals: An Overview

The instrument for which the Michelson objective was designed is a heterodyne interferometric profiler. It was originally designed for 10x or 20x magnified examination of test surfaces using a Mirau objective. (See Figure 2). As is apparent in the drawing, the Mirau interferometer suffers from increasing obscuration as the numerical aperture (N.A.) decreases relative to the angular subtense of the reference surface from the test surface. When using readily available microscope objectives (in which the numerical aperture usually decreases with magnification) it is therefore necessary to use a different kind of interference objective than the Mirau at low magnification.

Conventional microscope components in the profiler reimage the surface under test onto a linear array which detects the fringe pattern in one dimension. A sophisticated fringe interpretation system shifts

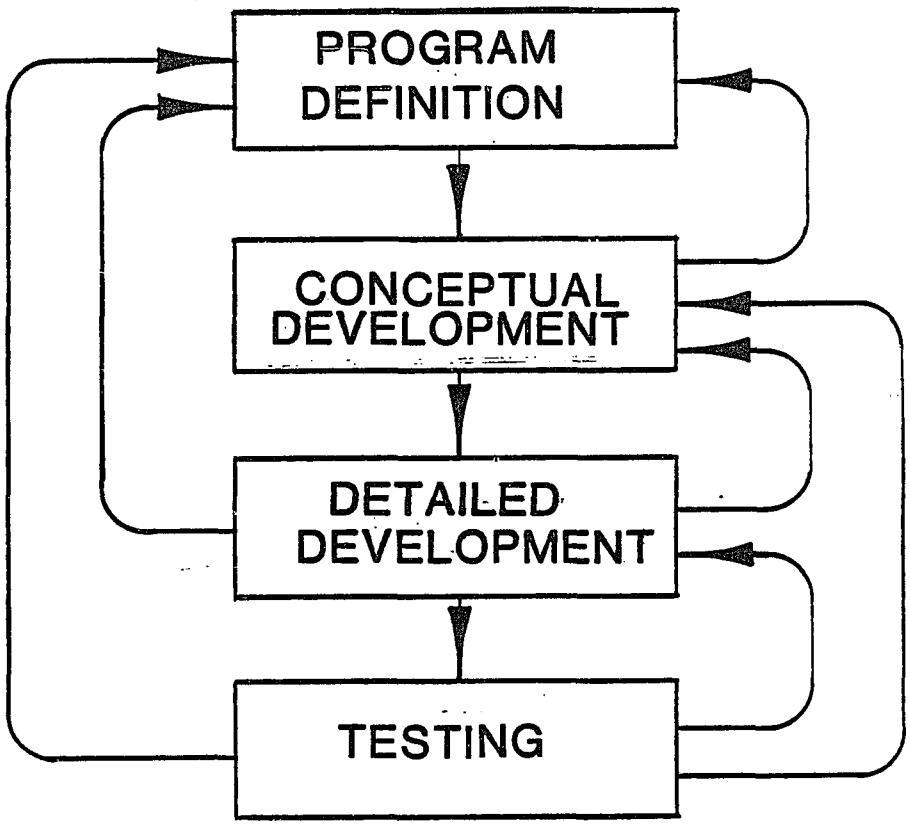

Fig. 1. Design Cycle.

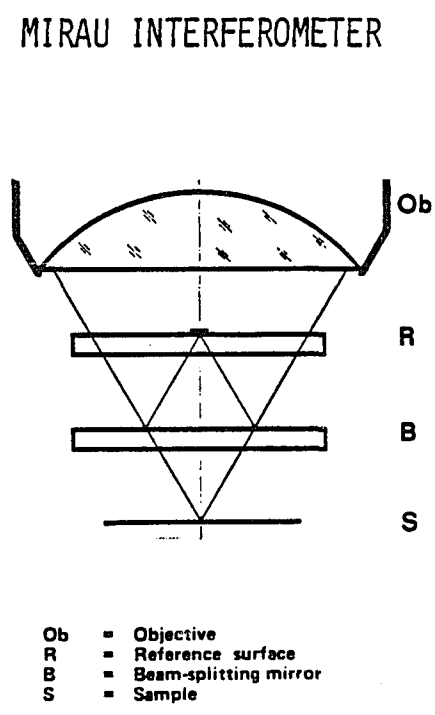

Fig. 2. Mirau Interferometer.

the Mirau interferometer vertically at constant speed while integration takes place in the detecting elements of the array. The algorithm which converts the irradiance pattern at the detector into a surface profile uses the "integrating bucket technique," in which absolute phase modulo 2π is calculated for each pixel of the detector (Wyant, 1983-84). (By "absolute" it is meant that there is no ambiguity in the fringe pattern as to whether a given slope is positive or negative.) After the one-dimensional irradiance pattern has been converted to phase information a microcomputer calculates the resulting surface profile. The length of the profile at the test surface is 1.3 mm for the 10x objective and .65 mm for the 20x objective. Figure 3 shows the optical schematic of the profiler.

Since the present system shifts the interferometric objective as a unit it is simplest to attach a new objective to the piezoelectric transducer (PZT) in place of the Mirau objective. The new assembly should contain a reference surface, appropriate interferometric components, and certain other refinements which grow out of the detailed examination in the following section. It should be reasonably light, compact and easy to operate.

A field diameter of five mm at the detector was chosen to characterize certain interesting surfaces which have lower spatial frequencies than the present system can study. Magnification of 2.5x meets this requirement nicely and has the added advantage of being available off-the-shelf from Nikon in a flat-field long working distance metallurgical microscope objective of .075 N.A.

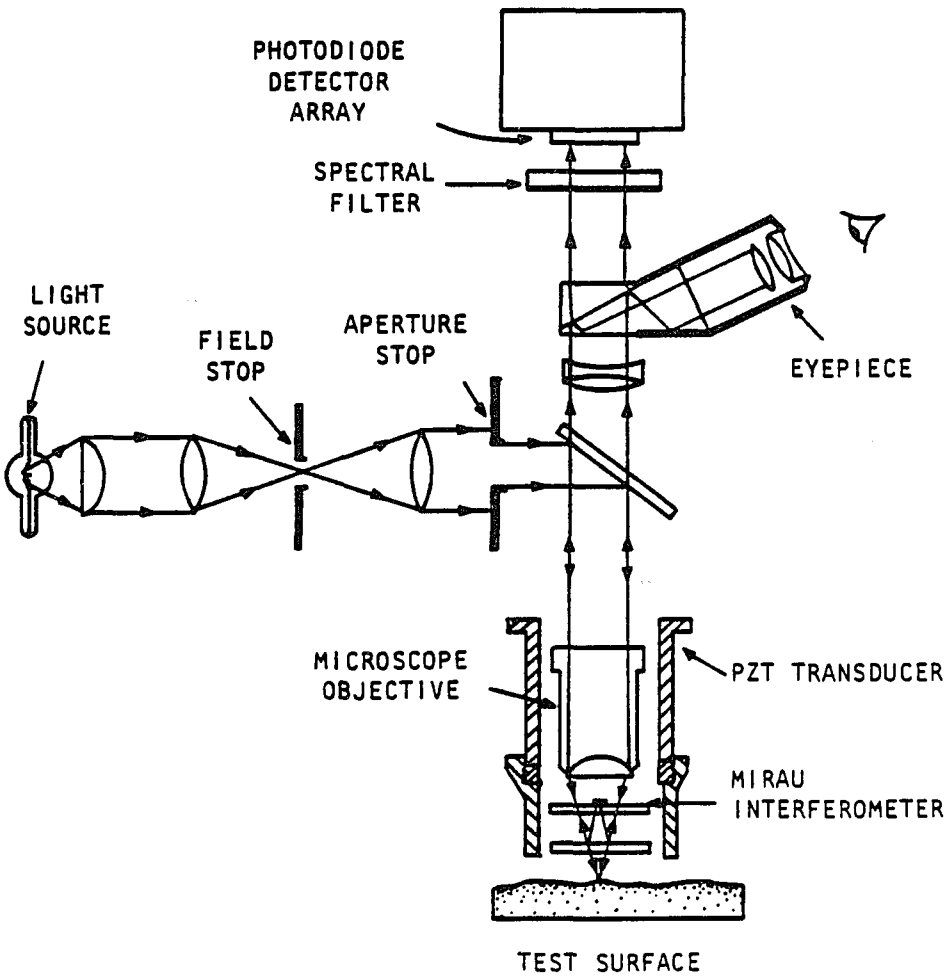

Fig. 3. Wyko Profiler.

In summary, the broad design goals describe a compact, lightweight interferometric attachment based on the Nikon 2.5X metallurgical objective. This device should be mechanically and optically compatible with the existing profiling microscope, and meet other yet-to-be specified requirements which will grow out of a closer look at the application. The following section will detail the development of the final configuration, extend the list of design features and model the performance of the finished objective.

CHAPTER 2

TWO BEAM EXTENDED SOURCE INTERFEROMETRY

Two Beam Interferometry

Assume two polarized plane waves in scalar form (Wyant, 1983-84):

$$A_1(x,t) = R_e[A_1 e^{i(\omega_1 t - k_1 x + \alpha_1)}] = A_1 \cos(\omega_1 t - k_1 x + \alpha_1)$$

$$A_2(x,t) = R_e[A_2 e^{i(\omega_2 t - k_2 x + \alpha_2)}] = A_2 \cos(\omega_1 t - k_2 x + \alpha_2)$$

Where A_1, A_2 are amplitude constants, $k = \frac{2\pi}{\lambda}$, $\omega = 2\pi\nu$ and α is a phase factor included for generality, and we assume that the two sources are coherent, i.e.

$$k_1 = k_2,\ \omega_1 = \omega_2,\ \lambda_1 = \lambda_2$$

Since the irradiance E is proportional to A^2 and since we average over many cycles because of the slow response of the detector,

$$E = \frac{1}{T}\int_t^{t+T} CA^2(x,t)dt = \frac{CA^2}{T}\int_t^{t+T} \cos^2(kx-\omega t+\alpha)\, dt = \frac{CA^2}{T}$$

where C is a constant of proportionality.

The amplitude resulting from the addition of two plane waves is

$$A_1(x,t) + A_2(x,t) = R_e\left[A_1 e^{i(\omega t - kx + \alpha_1)} + A_2 e^{i(\omega t - kx + \alpha_2)}\right]$$

Therefore

$$E = \frac{C}{T}\int_t^{t+T} [A_1^2 + A_2^2 + A_1 A_2 e^{i(\omega t - kx + \alpha_1)}\ e^{-i(\omega t - kx + \alpha_2)}$$

$$+ A_1 A_2\ e^{-i(\omega t - kx + \alpha_1)}\ e^{i(\omega t - kx + \alpha_2)}]\ dt$$

$$= I_1 + I_2 + 2\sqrt{I_1 I_2}\cos\ (\alpha_1 - \alpha_2)$$

where $2\sqrt{I_1 I_2}\cos(\alpha_1 - \alpha_2)$ is an interference term depending on the relative phase produced between wave trains at a given point. In the special case where $A_1 = A_2$ we have a sinusoidal pattern of bright and completely dark fringes expressed as a function of $(\alpha_1 - \alpha_2)$, the phase angle betwen wave trains at some point of observation.

If $A_1 \neq A_2$ the trough of the sinusoidal modulation does not go to zero; in this case the varying part represents some fraction of the average value. The fringe visibility is defined as:

$$V \equiv \frac{E_{max} - E_{min}}{E_{max} + E_{min}}$$

In order to observe an interference pattern $(\alpha_1 - \alpha_2)$ must vary slowly in time compared to the integrating time of the detector. The variation of $(\alpha_1 - \alpha_2)$ spatially will determine the shape of the fringe pattern and, given knowledge of the underlying geometry of the system can yield information about the shape of the incident wavefront. Conversely, if the image forming and wavefront properties are well

known, the shape of the fringe pattern can be used to analyze the geometry of the surfaces which produce it. This latter case describes the profiler.

Fringe Formation with an Extended Source

A useful model for studying two-beam interferometers is a conceptual version of the interferometer which superimposes the spaces of the two surfaces (Shack, 1982-84). (Figure 4). As will be seen later, this model is useful in explaining other two-beam interferometers. In this model two surfaces, S_1 and S_2 are placed in close proximity (separated by a distance smaller than the temporal coherence length of the source, which is approximately $\lambda^2/\Delta\lambda$). If the source of the illumination of the surfaces is extended, i.e. made up of a collection of independent point sources, it is clear that in order to observe interference it will be necessary to limit the variation of the optical path length for different pairs of rays arriving at a given point in the observation plane. One simple way of imposing this limit is by observing the real image produced at the focal plane of a positive lens. (Figure 5).

This technique is equivalent to mapping an angle in object space to a unique location in image space. The result is the selection of pairs of rays (one from each reflecting surface) which originate from the same point and which have a phase difference determined by the angle and displacement of the reflecting surfaces. It can be shown that a small displacement of parallel surfaces produces circular fringes. These fringes are called fringes of equal inclination, or

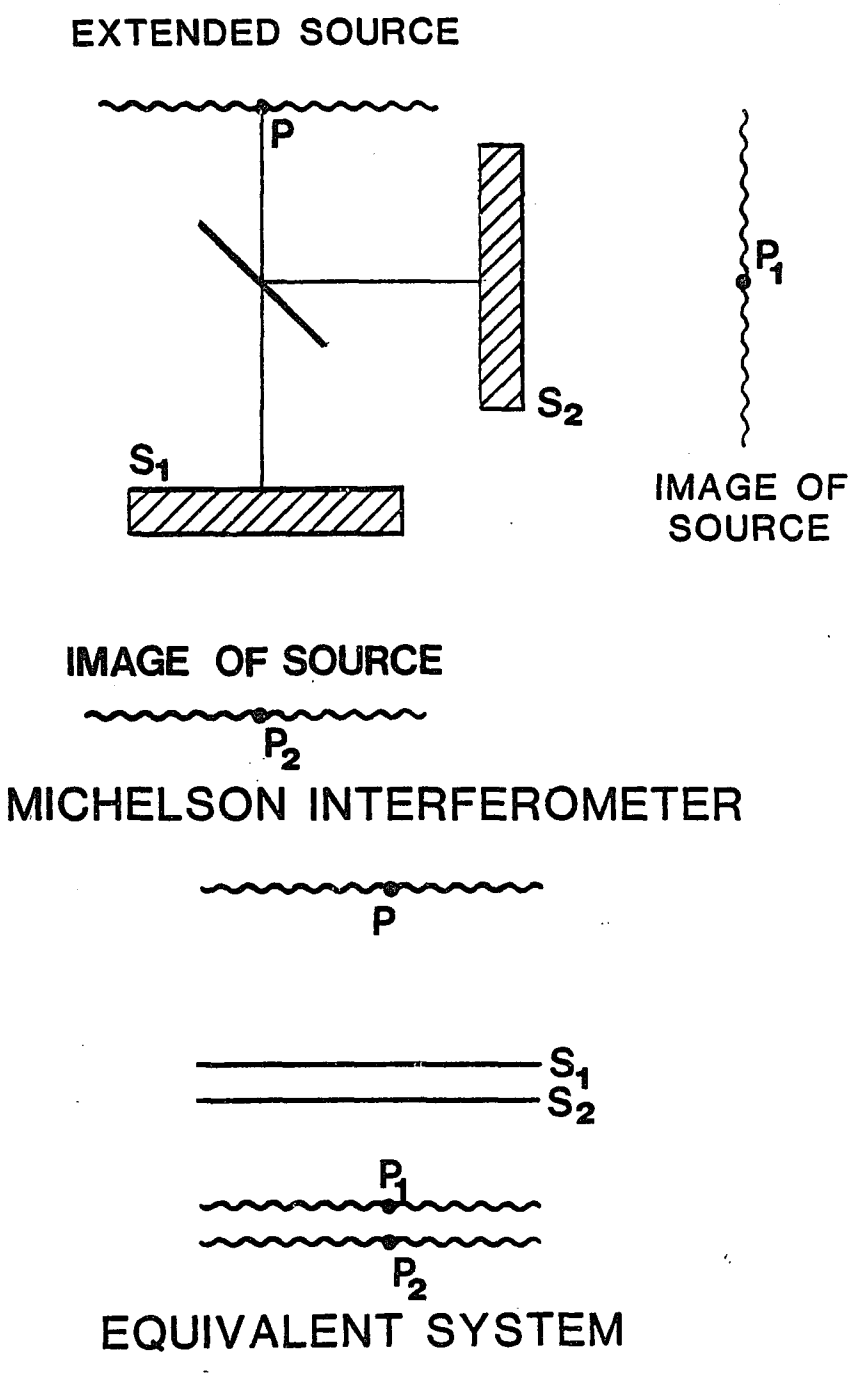

Fig. 4. Simplified Interferometer.

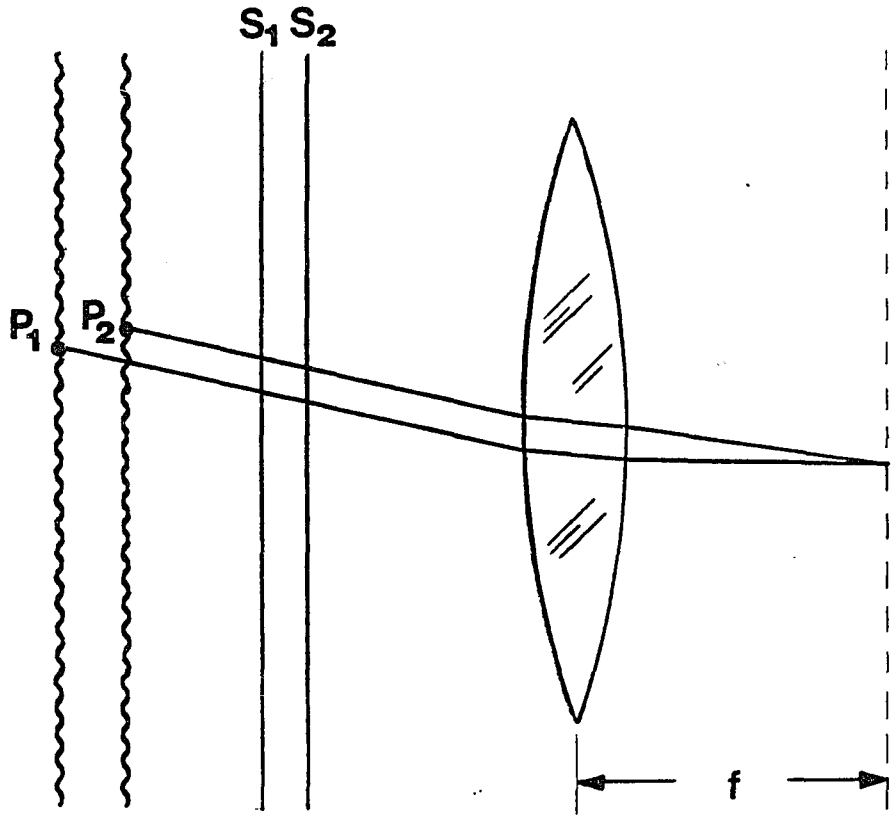

Fig. 5. Fringes localized at infinity.

Haidinger fringes, which are said to be localized at infinity since the image plane is conjugate to a plane an infinite distance away.

A second technique uses a positive lens to map the surfaces together onto the image plane. If the surfaces are coincident in the object space of the lens except for a small relative tilt, the image of each point source is primarily displaced laterally and the fringes which result are hyperbolic; furthermore they are in register (i.e. the fringe pattern produced by each source point is in phase with all others) only at the surface of the mirrors. (Figure 6).

These fringes are therefore said to be localized at the surfaces being investigated because these surfaces are conjugate to the image (Hecht, 1974). The phase of these fringes is determined by the separation between the surfaces, and can be shown to produce a hyperbolic fringe pattern at the image plane with one straight fringe corresponding to the line of intersection of the two superimposed surfaces. If in addition the source is removed to a great distance by suitable illuminating optics, all of the hyperbolic lines become straight in the limit. These fringes are called fringes of equal thickness since their phase is proportional to the distance between the superimposed surfaces. Fringes of equal thickness are particularly easy to interpret for surface profile information since they produce a sinusoidally modulated pattern whose phase is proportional to the height difference between a reference surface and the tested surface.

Succeeding sections show the Mirau, Mach-Zehnder and Michelson interferometers. As used for investigation of surface contours they

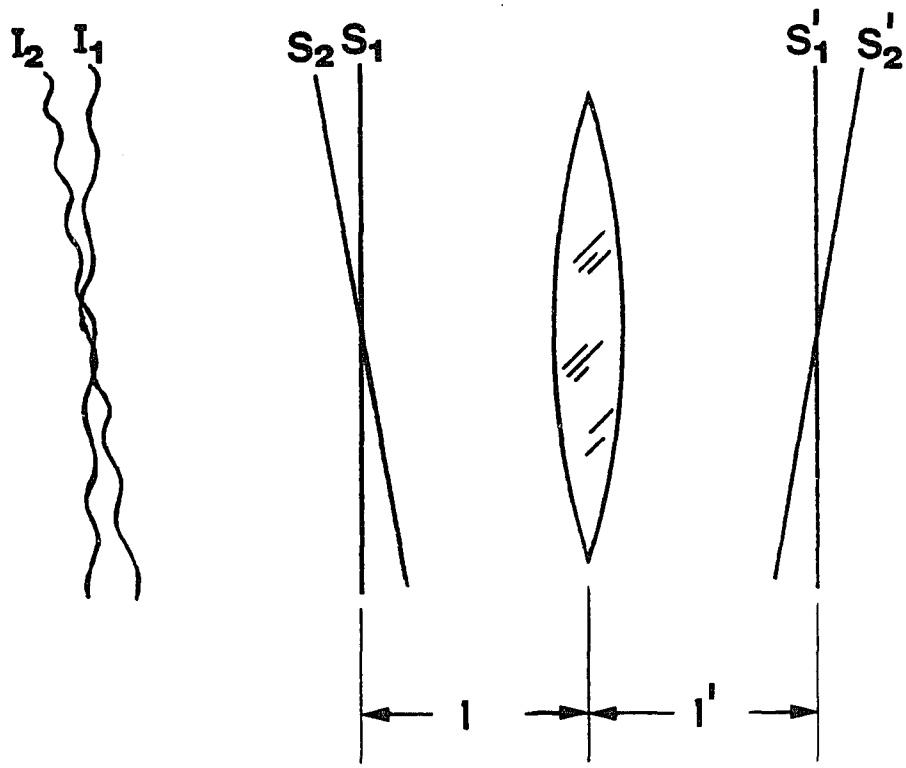

Fig. 6. Fringes localized at the surface.

have the common conceptual basis discussed above. All are capable of producing fringes of equal inclination or of equal thickness, although the Mirau would have a central obscuration problem and would need to be designed with a small amount of path difference between the two "arms." Each has its unique advantages and disadvantages as described below.

Choice of Interferometer Type

In choosing the type of interferometer for this project it was possible to correct some shortcomings of the Mirau. These include the following: (1) Lack of access for changing the reference surface; (2) relatively short working distance of the objective interferometer combination; (3) loss of contrast when viewing test surfaces of substantially different reflectivity than the reference surface; (4) difficulty blocking the reference beam when focusing the microscope objective on the test surface; and (5) limitations at lower values of magnification, as previously discussed. Primarily to insure compatibility with the existing device the choice of interferometers is limited to amplitude-splitting types. Of these there are many types but the Michelson is the prime candidate; a similar type, the Mach-Zehnder interferometer, is also worth discussion if only because of an interesting similarity to the Mirau which will be discussed below.

The Michelson interferometer (Figure 7) makes it relatively easy to solve the above problems because its reference surface is perpendicular to the optical axis. Partly because of the use of a lower power objective with longer working distance and partly because

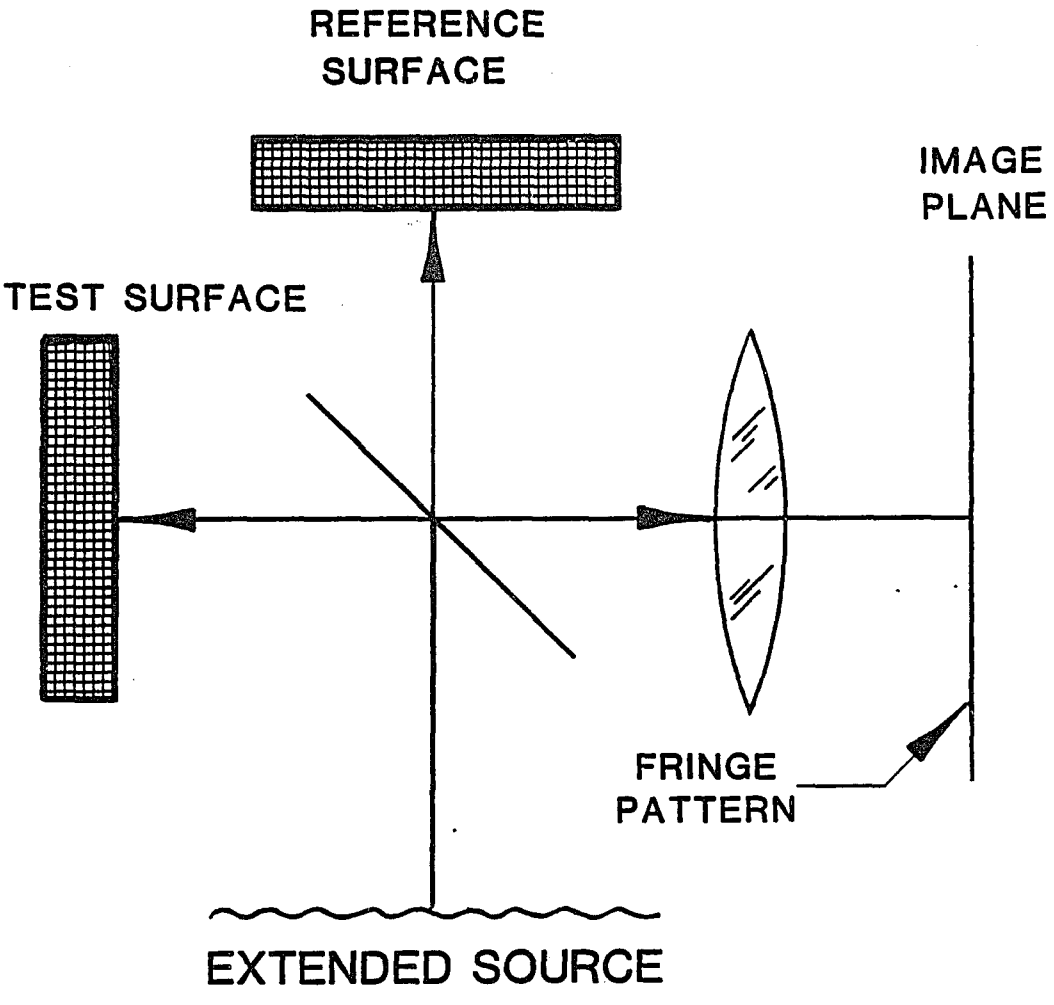

Fig. 7. Michelson Interferometer.

of the inherently more "open" geometry of the Michelson configuration, all of the above problems can be eliminated or ameliorated. Moreover, this particular geometry opens up some unforeseen possibilities for increasing the utility of the system. For example, the relatively large volume surrounding the beamsplitter will easily accommodate not one, but three selectable reference surfaces which can represent different curvature or reflectivity. Since the reference surface is easily accessible, it is practical to enclose these reference surfaces in cartridges which are easily changeable by the operator, thus adding utility and flexibility to the basic instrument. Additionally, since the Michelson configuration has symmetry with respect to the reference and test surfaces, it is possible to interchange them and look sideways to the test surface. This configuration is particularly useful for inspecting the insides of such surfaces as bearing races, deep conics, and so on.

The Mach-Zehnder interferometer is worth mentioning if only for the insight which it lends to the Mirau instrument. (See Figure 8). If we take the basic form (Figure 8-a) and rotate it (Figure 8-b) we see that the reference surface and the test surface are not only parallel to each other but adjacent. If we extend and connect the separate beam splitters and add an imaging system of relatively large N.A. "looking around" the reference surface, we have come full circle to the Mirau interferometer (8-c). The Mirau interferometer can be seen as a version of the Mach-Zehnder interferometer (or vice versa, which ever the reader prefers).

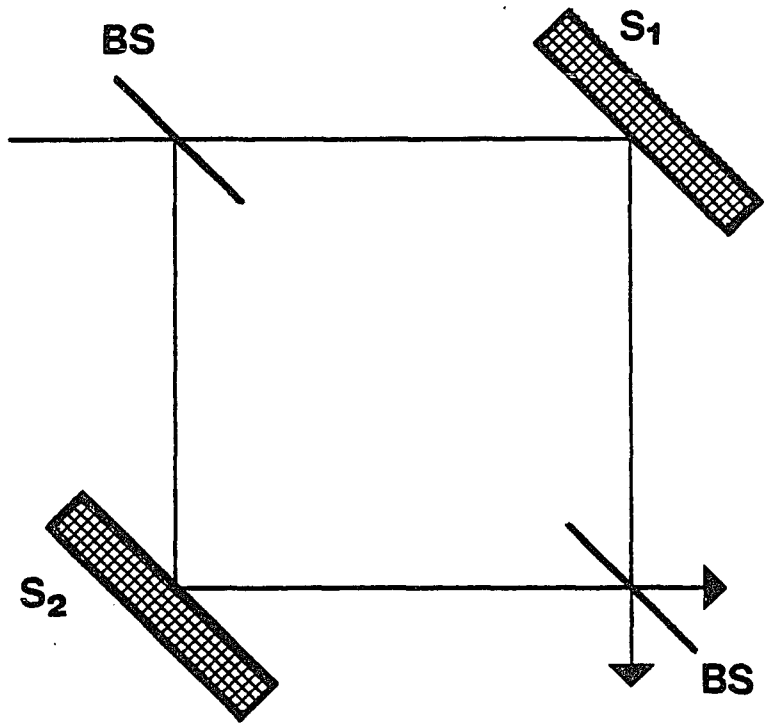

(a)

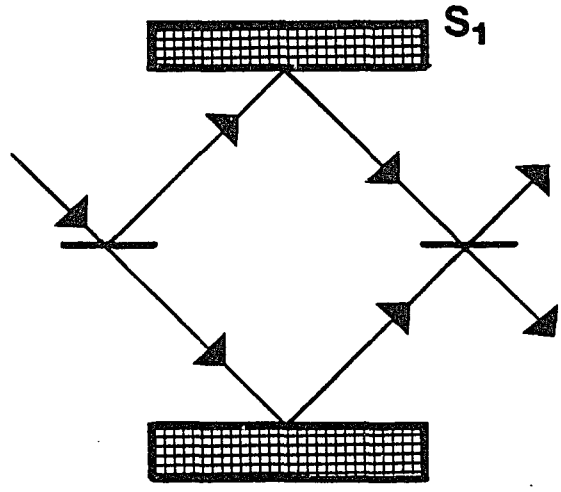

(b)

Fig. 8. Mach-Zehnder and Mirau interferometers.

(a) and (b) Mach-Zehnder Interferometer.

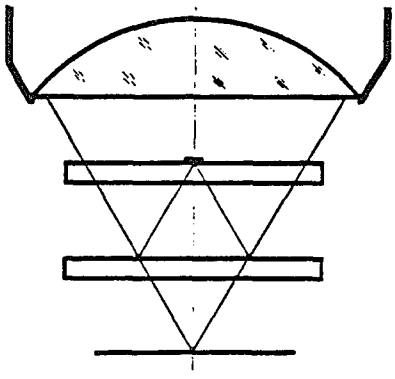

(c)

Fig. 8. (Continued) Mach-Zehnder and Mirau interferometers.

(c) Mirau interferometer.

Physical Optics Design Considerations

The Michelson and the Mirau interferometers share some common principles which it will be helpful to summarize before going further into the development of the Michelson version. Both use extended light sources and therefore require that the optical path through both arms of the interferometer be equal. This requirement seems at first glance to be a fault of these systems; the question is often asked, "Why not use a HeNe laser and eliminate all the fuss about optical path differences?"

The main result of using a source of greater coherence length would be the introduction of large numbers of spurious interference fringes into the output at the detector: sources of reflection and diffraction in the system, rather than simply causing a slight decrease in the contrast of the desired fringes, would introduce a host of new fringes. While interpreting the resulting pattern for profile information would be theoretically possible, it would be more difficult and would certainly yield a result of much lower signal-to-noise than that obtained with an extended source.

A minor limitation of this class of interferometer is imposed by the coherence length of the source: namely that the phase shift created by the PZT be small in comparison to this coherence length. This is not really a handicap since the phase interpolation algorithm requires a total phase shift of less than one wavelength, whereas the coherence length of the source is seen to be approximately

$$\frac{\lambda^2}{\Delta\lambda} \approx \frac{.6^2}{.2} = 1.8\ \mu m \text{ or about } 3\lambda.$$

Since the coherence length of the source is just a few wavelengths it is important that the optical path length in the two arms must be equal to within approximately this tolerance. Optical path length is defined by

$$O.P.L. = ns$$

(where **n** is the refractive index of the transmitting medium and **s** is the geometrical distance). This requirement is met in both the Mirau and the Michelson by adjusting the location of the test surface so that the O.P.L. of the distance between it and the beamsplitter is equal to the O.P.L. of the distance between the beamsplitter and the reference surface. However, since the refractive index **n** varies with the wavelength of the incident light, and since interferometric beamsplitters have appreciable thickness, dispersion in the beamsplitter material will cause a wavelength-dependent phase shift which, unless it is exactly matched in both arms of the interferometer, will reduce the contrast of the fringes. Therefore any part of the beamsplitter in one arm of the interferometer must be compensated by an element of similar optical properties in the other arm to avoid loss of contrast to dispersion. As will be shown in the following section, dispersion places one of the most stringent requirements on the quality of the beamsplitter.

CHAPTER 3

DESIGN DEVELOPMENT

Sensitive Parameters

The optical profiler is an exquisitely sensitive instrument for measuring profiles at the surfaces of suitable materials. Vertical resolution averaged over the area imaged onto each individual pixel of the detector (area approximately 1.3 micrometer x 1.3 micrometer) can approach 0.1 nanometers under good conditions (mechanical isolation, very smooth samples). This distance is just a little more than 1/10,000 of the wavelength of red light!

Changing the magnification of the microscope objective changes lateral resolution and the length of the profile studied, but it does not change the vertical resolution. Any mechanical perturbation or optical aberration introduced into the system can obviously have disastrous consequences for the accuracy, precision and repeatability of such measurements. It is therefore important to develop an understanding of the stability and sensitivity of the proposed system, and to model the sensitive parameters carefully enough to be able to predict system performance with confidence. Otherwise the design process will at best be an expensive after-the-fact exercise in problem solving.

The following discussion reviews a number of mechanical and optical parameters with regard to their effect upon the quality of

wavefront measurements. The list is derived from geometrical and physical optics, more or less obvious mechanical concerns, optical breadboard models of the system and experience with the present Mirau profiler. Its objective is not only to reveal the pitfalls but hopefully some unexpected opportunities for increasing the utility, economy and elegance of the design.

Mechanical Considerations

The PZT surrounds the objective in the Mirau microscope because it is the most convenient place to put the rather long cylindrical housing. It is therefore more practical to translate the entire Mirau assembly relative to the test sample rather than to move just the reference surface. The same geometrical considerations apply to the Michelson version because it is important to keep the radius of the interferometer envelope to a minimum for working inside curved surfaces. (Figure 9).

If the configuration of Figure 7 is employed using a long working distance microscope objective and a cube beamsplitter whose halves are well matched, the result is a compact Michelson interferometer. Insertion of the beam splitter into the direct beam extends the working distance by

$$\frac{(n-1)d}{n}$$

where **n** is the refractive index and **d** is the thickness of the cube. The O.P.D. is increased by

$$\frac{(n-1)d}{1 + 1/n}$$

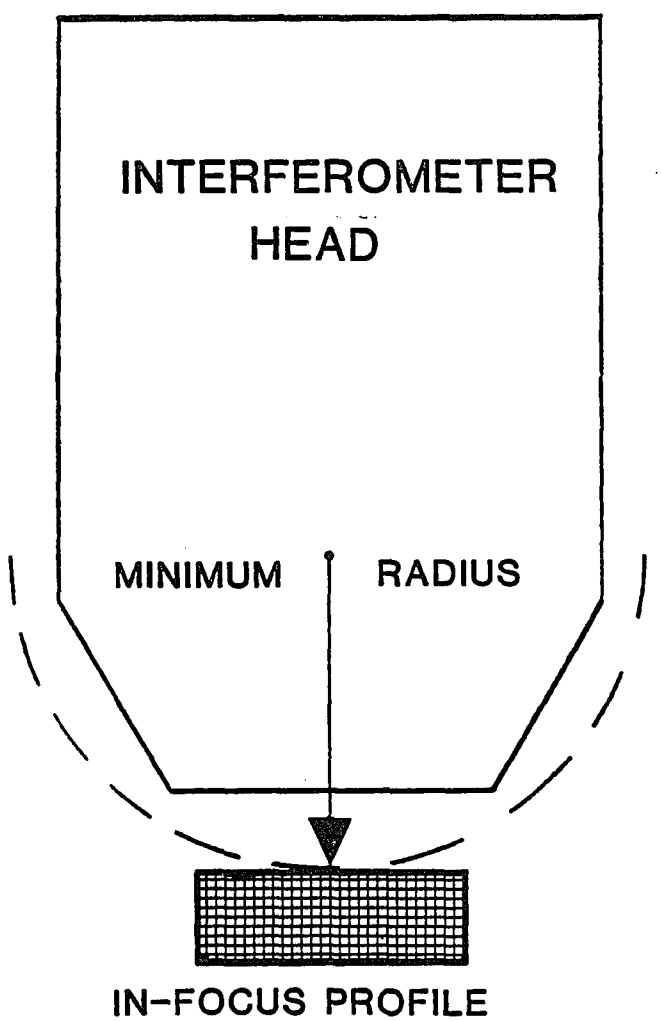

Fig. 9. Minimum radius of curvature envelope.

the test beam meets the test surface (tip-tilt). From the operator's standpoint the angle must be smoothly controllable through small angles. To estimate the sensitivity required we use the equation for fringe spacing when interfering two plane waves. (Figure 10).

If we assume an adjusting arm of approximately 1" length a displacemnt of .001" would be required to remove 10 fringes of tilt. For an 80 TPI (threads per inch) adjusting screw this is a rotation of 30 degrees.

There are two primary options for obtaining the two degrees of angular freedom required for tip-tilt adjustment. For both methods the center of curvature of the motion must be at an image to prevent mismatch of the O.P.L. (usually misnamed "defocus") with consequent loss of fringe contrast. In the first there is a rotatable plate which moves together with the beamsplitter and reference. This method has been used commercially by Leitz, but has the disadvantage of introducing off-axis aberrations into the combined beam; this method also requires a rather awkward disassembly procedure for changing reference surfaces. (Figure 11).

The second method is simpler and more flexible and indeed is the key design concept which generated the form of the solution. It employs angular contact spherical bearings which can be adjusted along their axes to place their centers of the curvature at the focal plane of the reference beam. Threaded cartridges screw into the male bearing seats. These cartridges also are adjustable so that reference mirrors can in turn be placed at the center of the curvature of the bearing.

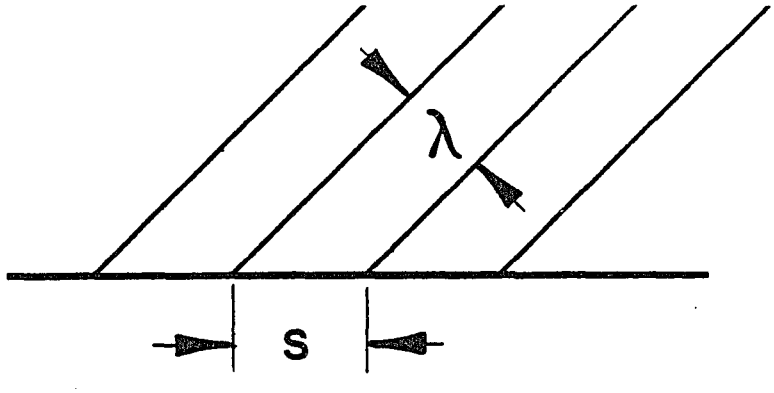

$$S = \frac{\lambda}{\sin\theta} \simeq \frac{\lambda}{\theta}$$

$S = .5$ mm $\quad \theta \simeq .001$ (10 fringes across field)

Fig. 10. Tip-tilt sensitivity.

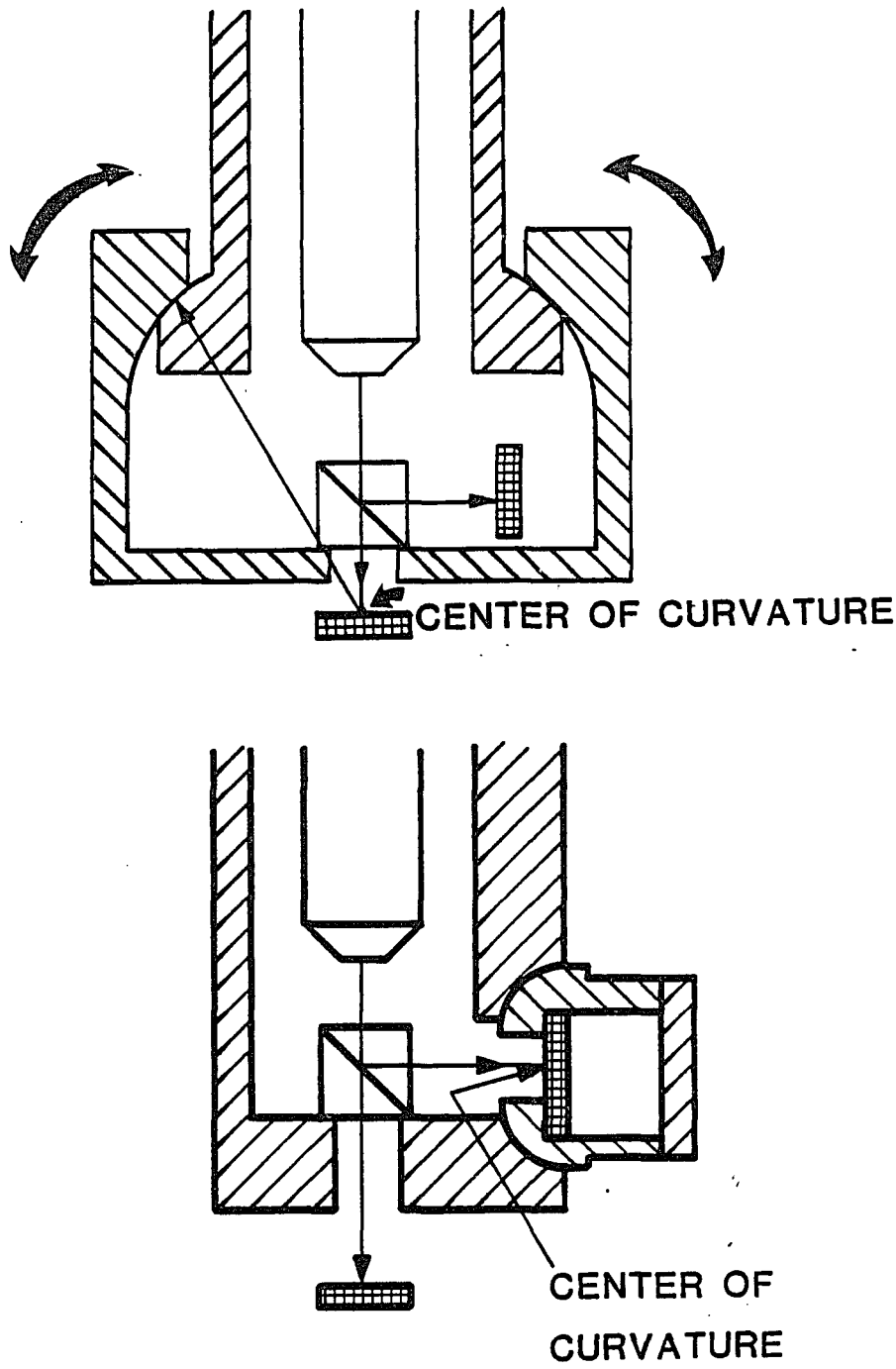

Fig. 11. Tip-Tilt Options.

The adjustability of the cartridge not only eases production tolerances but also makes it possible to install curved reference surfaces for testing complex shapes.

Aberrations

Aberrations can affect profile measurements in two related but slightly different ways: first by introducing differential path changes into the separate beams to the test surface and the reference mirror, and second by changing the combined path of the beams from the surfaces to the detector array. Differential effects change either the visibility of fringes because of the limited coherence length of the light source, or the shape of the fringes through the introduction of non-symmetrical phase shifts in the separate arms. Common path effects not only govern the quality of the image projected onto the detector, but surprisingly can also change the shape of the fringe pattern, thereby introducing errors into the profile measurement.

The first effect depends only on the difference between the path travelled by the separate beams; the identical halves of an ideally symmetrical beamsplitter would exactly cancel any introduced path differences. For white light fringes dispersion imposes a rather stringent limitation on the alignment of the halves of the beamsplitter cube. The following calculations are used to generate a preliminary tolerance limit for alignment of the beamsplitter halves based on dispersion effects. Subsequent discussion will examine the effects of other aberrations in the beamsplitter followed by a discussion of the second set of effects, revealing a somewhat surprising additional

requirement on the microscope objective (telecentricity).

Dispersion and Visibility

Since focus is adjustable in the profiling microscope we assume that focus and piston errors in the separate paths cancel, except for the effects of dispersion. Assume, furthermore, a spectral range of .4047 micrometers to .7665 micrometers. If we adjust optical paths to be equal at some wavelength, say .7665 micrometers, then for a $\Delta\lambda$ of .3618 micrometers we limit O.P.D. to be $\lambda/4$. (Figure 12). There are two contributions to O.P.D.:

1. Longitudinal displacement of the image.

$$OPD \simeq \Delta\ell = \frac{n-1}{n} \quad T$$

2. O.P.D. caused by propagation through the glass (piston error).

$$OPD = (n-1)\ T$$

Adding, we get

$$O.P.D. = \left[(n-1) + \frac{n-1}{n} \right] T = (n - \frac{1}{n})T$$

using data from Modern Optical Engineering, (Smith, 1966) for BK7

$$n_h \ @ \ .4047\ \mu m = 1.53043$$

$$n_{A'} \ @ \ .7665\ \mu m = 1.51179$$

$$\Delta\ O.P.D. = 2\left[\Delta n - \Delta\ (\frac{1}{h})\right]\Delta T = \frac{\lambda}{4}$$

$$\Delta T = 3.5\ \mu m$$

where ΔT is used since we are interested in the difference between the two paths. The factor of two results from the doubled path in the interferometer. This is a rather conservative calculation because of

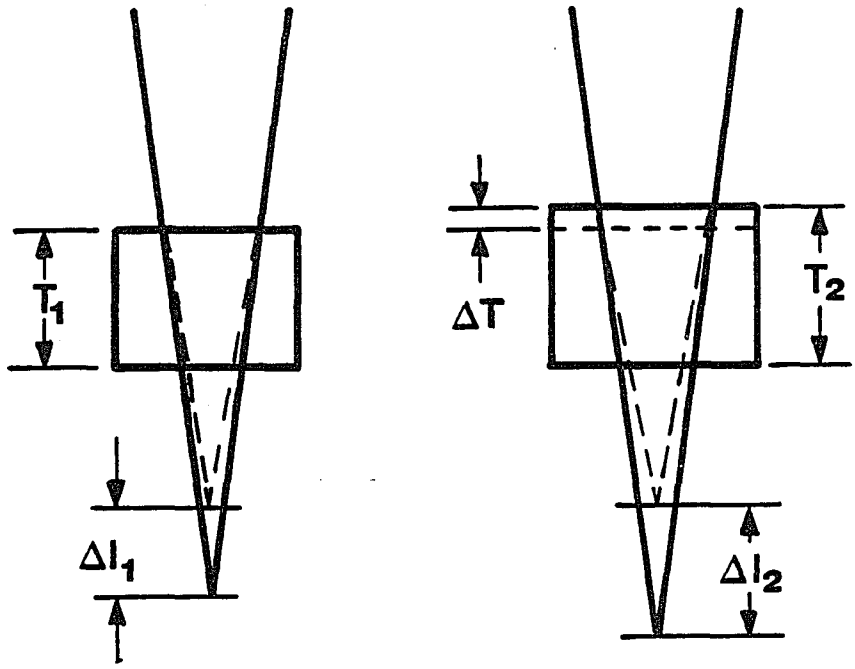

Fig. 12. Dispersion and visibility.

the use of a $\lambda/4$ criterion and the rather wide spectral range. If we use

$$\lambda_f = .4861\ \mu m, \quad n_f = 1.52262$$

$$\lambda_C = .6563\ \mu m, \quad n_c = 1.51461$$

we get

$$\Delta T \approx 7\ \mu m$$

Measured values in the lab agree well with these calculated values. A prism with misalignment of less than 5 micrometers had a measured visibility better than .90. For construction purposes, then, it is clear that alignment of the prism halves will be a sensitive parameter.

Other Beamsplitter Aberrations

In similar applications beamsplitter aberrations are sometimes ignored on the assumption that "averaging" over the beam will remove aberration-induced phase shifts. This assumption is valid if the correlation length of aberrations in the beamsplitter is small compared with the projection of the beam, or if all beams pass through the same area of the beamsplitter. Placing the beamsplitter at the pupil of the imaging system would meet the latter requirement but only at the cost of losing control over placement of the stop to control other aberrations. As will be shown later, this would be an unwise choice. It is therefore necessary to inquire into the limitations imposed by following the first course of action.

Beamsplitter aberrations can originate from surface imperfections at the faces or the hypotenuse, from inhomogeneities in the glass, or from mechanical stresses introduced by gluing the halves

of the beamsplitter together; these aberrations can add together in unpredictable ways. For these reasons it is probably not useful to try to model beamsplitter aberrations other than to say that all aberrations at all orders may be present in any given beamsplitter. It is clear, however, that those imperfections which have spatial frequencies which are short compared to the marginal ray height at the beamsplitter will primarily contribute to loss of visibility in the fringe pattern, while those which have characteristically longer spatial frequencies will distort the shape of the fringe pattern. (Figure 13.)

An interesting special case is the one involving zero spatial frequency. The lateral misalignment discussed in connection with dispersion as a wavelength-dependent shift in O.P.L. is important here in producing piston error which is linearly dependent on the chief ray angle.

Fringes localized at the surface now look like fringes localized at infinity! Since the O.P.D. is dependent on the cosine of the chief ray angle, any system which is approximately telecentric in object space will not show significant effects. Indeed, all aberrations (piston error, coma, astigmatism, distortion, field curvature and lateral chromatic) which depend on field height will affect the shape of the fringes unless the imaging system is telecentric. This is a somewhat surprising result in two ways: first that the imaging system, which is outside the interferometer cavity, can affect the shape of the fringes; and second, that a stop shift can not only improve common path effects, but also differential effects.

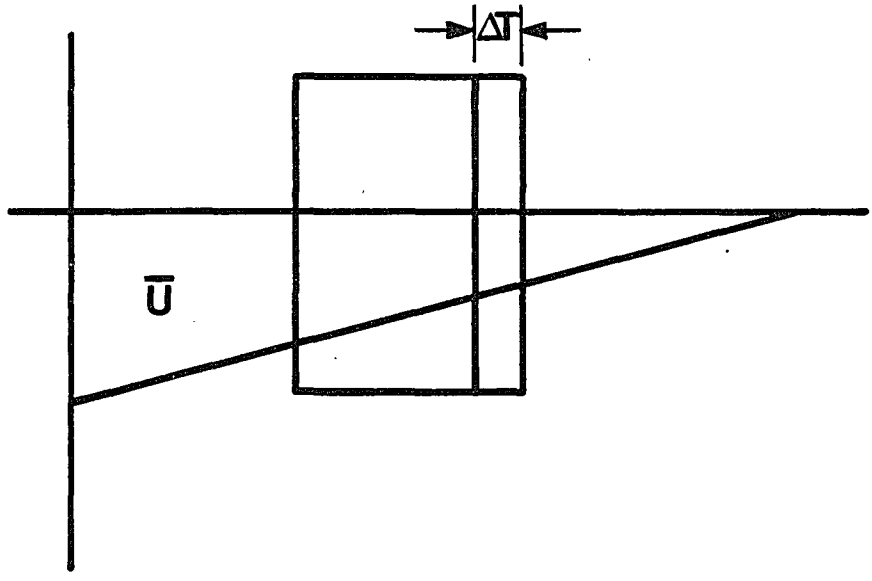

Fig. 13. Piston Error.

Because it is clear that the quality of the beamsplitter is very critical in this instrument the following method was developed for estimating the effect of wave front aberrations: if an interferogram of the beamsplitter, e.g. taken by a Zygo interferometer, is averaged over the projection of the beam at the beamsplitter the resulting wave aberration function will approximate the introduced aberrations. (Figure 14).

The effect of this averaging is to give some "leverage" on beamsplitter aberrations which, depending on the nature of the aberration, may be significantly less than the total aberration present in the beamsplitter as a whole. In this system the "leverage" value varies from about 0.1 to 0.25 depending on the behavior of the aberration with field height. In other words, one wave of coma in the beamsplitter appears to generate about 0.1 to 0.25 wave of coma in the profile.

While studying the interferogram a qualitative assessment of loss of visibility can also be made by studying the wavefront quality of different zones swept out by the beam projected on the beamsplitter. (Figure 15). Notice that it is possible for one part of the fringe pattern to have higher visibility than another part based on local variations in quality. (Figure 16).

Image Quality

Image quality is important primarily as it affects the lateral resolution of the detector through increase of the point spread function size, and the vertical resolution of the system through

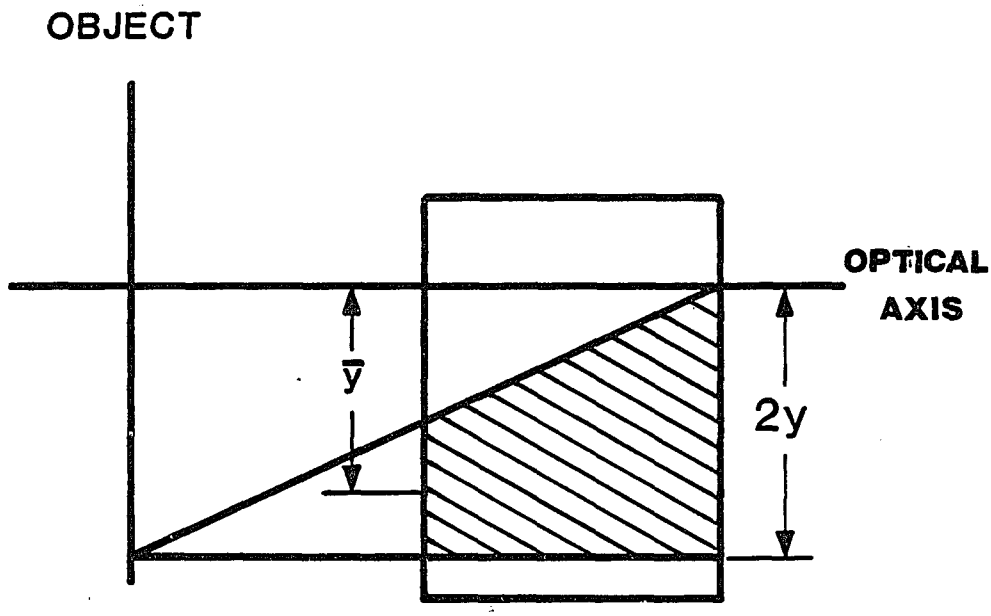

Fig. 14. Extent of averaging over cube beamsplitter.

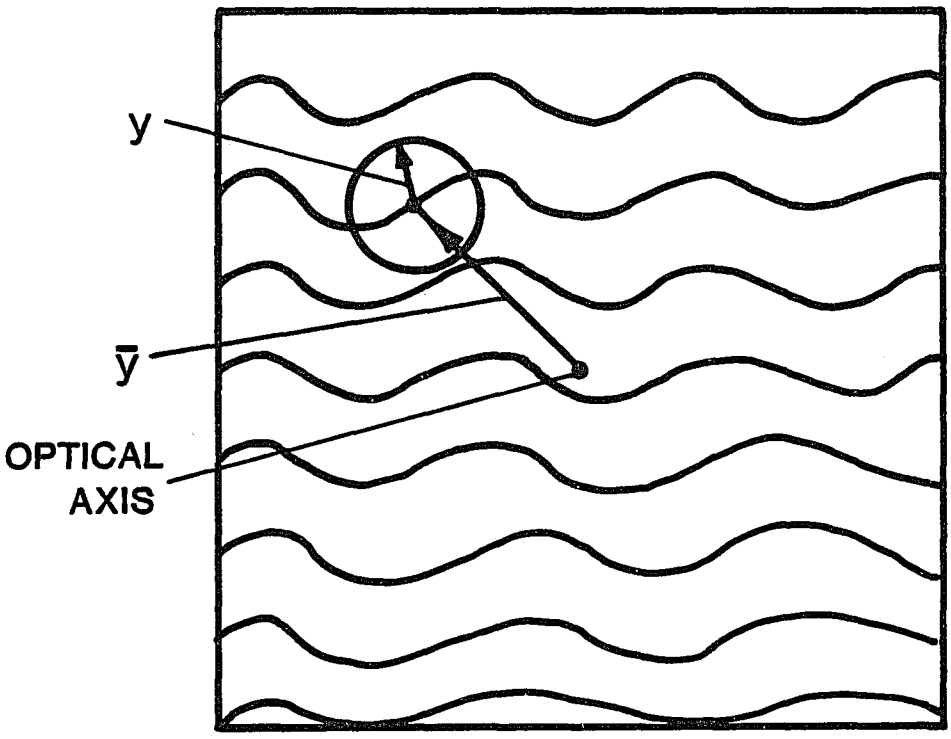

Fig. 15. Estimating the effect of partial averaging.

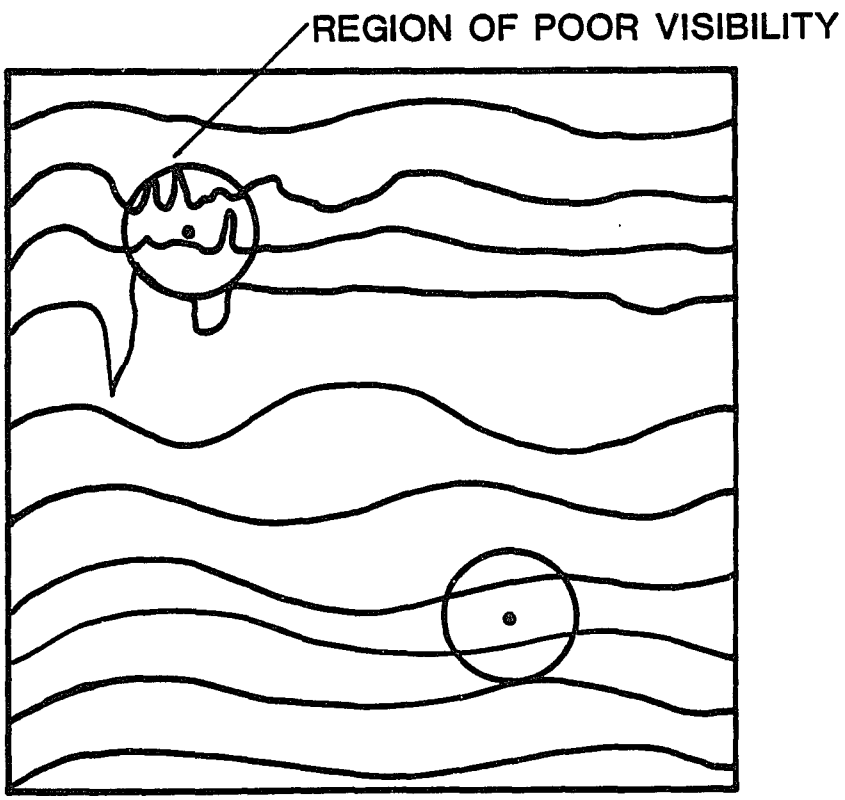

Fig. 16. Wavefront aberrations within the averaged area.

reduction of signal-to-noise ratio at higher spatial frequencies. In determining the effects of aberrations there are three main approaches which can be followed:

1. Analyze the effects with computerized numerical tools.
2. Analyze the effects according to classical aberration theory.
3. Build the system and measure the aberrations using standard testing techniques.

The first method was postponed in its complete form because of the difficulty of acquiring Nikon's lens prescription, combined with the author's lack of access to, and facility with, the computer modeling tools; in the end this analytical power proved unnecessary because of the simple nature of the problem. A combination of methods two and three was used: first, to show that the problem was manageable; and second, to include real deviations of the actual hardware from theoretical specifications (tilt, decenter, etc. of system components). Specifically it was shown that third order aberrations are within reasonable limits for good image quality. After construction, appropriate testing was done to check total system performance.

The following calculations are based on the use of structural aberration coefficients and surface-by-surface Seidel coefficient contributions as developed in Professor Roland Shack's two introductory courses in optical analysis and design at the University of Arizona Optical Sciences Center (Shack, 1982-84). First order system properties are summarized in Figure 17a-17b.

The following approach is a surface-by-surface calculation of Seidel

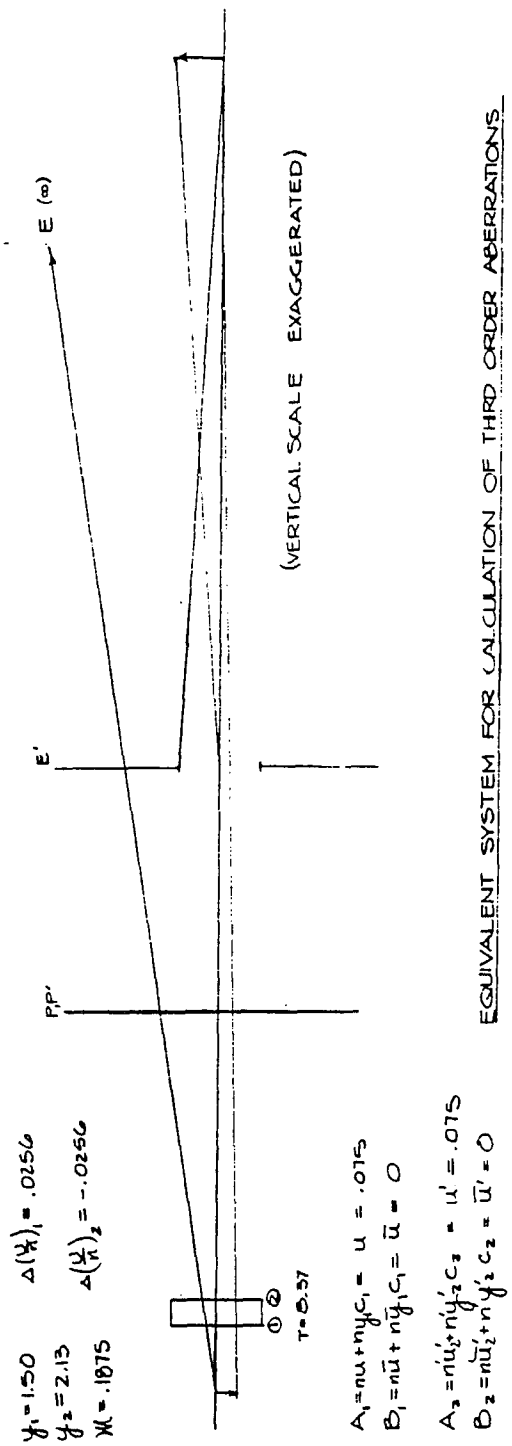

Fig. 17-a. First order properties.

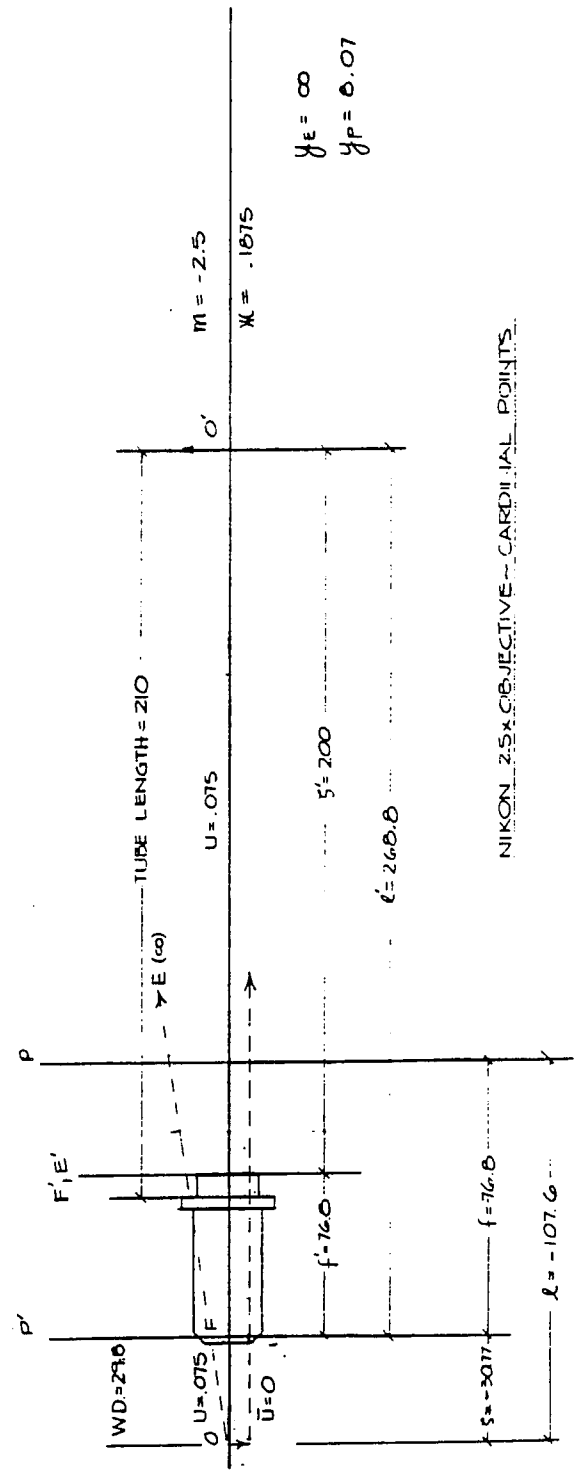

Fig. 17-b. First order properties (continued).

coefficients to third order for an idealized beamsplitter (no curvature). It is particularly insightful in showing the effects of telecentricity and, qualitatively at least, the influence of departure from flatness in the beamsplitter.

$$S_I = -\Sigma A^2 y \Delta \left(\frac{u}{n}\right) \qquad A = nu + nyc$$

$$S_{II} = -\Sigma AB y \Delta \left(\frac{u}{n}\right) \qquad B = n\bar{u} + n\bar{y}c$$

$$S_{III} = -\Sigma B^2 y \Delta \left(\frac{u}{n}\right) \qquad P = C\Delta \left(\frac{1}{n}\right)$$

$$S_{IV} = -\Sigma H^2 P \qquad \frac{\delta n}{n} = \frac{n-1}{\nu n}$$

$$S_V = -\Sigma B/A \left[H^2 P + B^2 y \Delta \left(\frac{u}{n}\right)\right]$$

$$C_L = \Sigma A y \Delta \left(\frac{\delta n}{n}\right)$$

$$C_T = \Sigma B y \Delta \left(\frac{\delta n}{n}\right)$$

For this system $\bar{u} = 0$ and $C = 0$ (ideal beamsplitter). Therefore $B \equiv 0$ and S_{II}, S_{III}, S_{IV}, S_V and C_T vanish. The remaining terms are:

$$A = U = .075 \qquad S_I = -.00001751$$

$$\frac{\delta n}{n} = .005308 \qquad C_L = .0003297$$

In terms of wave aberration coefficients we have:

$$W_{040} = -.0022 \ \mu m \ (\approx \lambda/275)$$

$$W_{131} = 0$$

$W_{222} = 0$

$W_{311} = 0$

$\delta_\lambda W_{111} = .17\mu \ (\simeq \frac{\lambda}{4})$

By far the largest term is longitudinal chromatic aberration. This term has been treated earlier in combination with piston error under "Dispersion." This term has only a negligible effect as defocus since all images are still laterally in register at the image plane as a result of telecentricity in object space.

In summary it is clear that because of the low N.A. of this lens the pupil aberrations have acceptably low values. Telecentricity in object space eliminates all of the field aberrations for an ideal beamsplitter aligned with the optical axis, although even if the system were not telecentric these values would still be negligible in the formation of the image at the detector.

Summary of Requirements

In any design project a decision must be made which establishes a hierarchy of tradeoffs. The designer must find a way of reconciling the client's desires and the inherent (but sometimes not obvious) opportunities and constraints of the system itself. This section is a brief summary of the design goals.

Mechanical and Optical Properties

1. Long working distance.
2. Smallest possible mechanical envelope for tight places.

3. Multiple interchangeable reference surfaces.

4. Light, sturdy, simple.

5. Free of systematic errors which would need to be removed by calibration.

Optical Properties

1. Easy to use.

2. Difficult to damage.

3. Errors introduced by improper operation will be obvious.

4. Requires no different technique than present objective.

General

1. Inexpensive.

2. Interchangeable with present objective.

3. Uses standard, readily available components.

4. Establishes unique or novel, yet saleable capability.

5. Attractive, well packaged and finished.

Quid Pro Quo

The most important tradeoff in this design originates from the use of a thick beam splitter in a converging beam. By so doing the general problem is greatly simplified because a commercially available objective lens can be used without modifiction, and the number of optical components which are not common to both beams is kept to a minimum. On the debit side, however, the beamsplitter introduces some obvious and some not-so-obvious aberrations into the system. As a result the optical quality of the beamsplitter must be high, and the

microscope objective should ideally be telecentric in object space.

Mechanically the system has many degrees of freedom, subject to the usual constraints of interferometric devices: namely rigidity, great precision in alignment and smoothness of motion. Otherwise, however, there are many different configurations which would satisfy the basic requirements. Three are explored subsequently as drawings; one was built and tested.

CHAPTER 4

IMPLEMENTATION

Following are assembly drawings for three different versions of the Michelson interferometer objective. The first has three reference cartridges equidistant around the central housing in order to provide maximum flexibility for testing a variety of different kinds of samples. The second uses only one reference cartridge assembly to keep the overall mechanical size to a minimum. A variation of this version would use motorized control of tip and tilt for remote operation. The third is a side-looking version which can see inside surfaces not accessible to the other two. All three share the same basic optical configuration, i.e. a Michelson interferometer with fringes of equal distance localized at the surfaces of the test and reference mirrors.

This device was designed from the beginning to be a limited-run commercial product, fully interchangeable with other objectives on the basic instrument. Therefore all tolerances had to meet appropriate standards for interchangeability, materials had to be non-exotic in their availability and fabrication procedures, and construction and alignment of the completed system had to be simple and straightforward. The following sections describe the detailed implementation of these design considerations.

Tolerances

Standard practices for specifying tolerances were followed. Unified National thread specifications, appropriate dimensioning to control accumulation of tolerances and fully specified tolerance limits were incorporated in all drawings. Single point threading was used only when unavoidable and then only as controlled by the use of standard taps or dies for the matching parts. (Thread gauges are recommended for production inspection.)

Because the final device must be assembled to optical tolerances (e.g. equal O.P.D. to within a few wavelengths of light) and yet be achievable with standard machining practices, all critical parameters were designed to be adjusted in final assembly. Given this approach it was mainly important to assure that unavoidable imprecision would not (1) exceed available adjustment allowance; (2) exceed tolerances through lack of repeatability in operation; or (3) accumulate excessively through wear in use. Admittedly these guidelines require insight into a broad area of mechanical properties, generalized design experience and testing of the finished product for successful implementation; nevertheless there are some design techniques useful in controlling these problems, as discussed in the following sections.

Mechanical Layout

The three-mirror version (figure 18) requires a beamsplitter cube holder which moves easily, stops at a repeatable location and angle, and supports the cube firmly during measurements. All of these

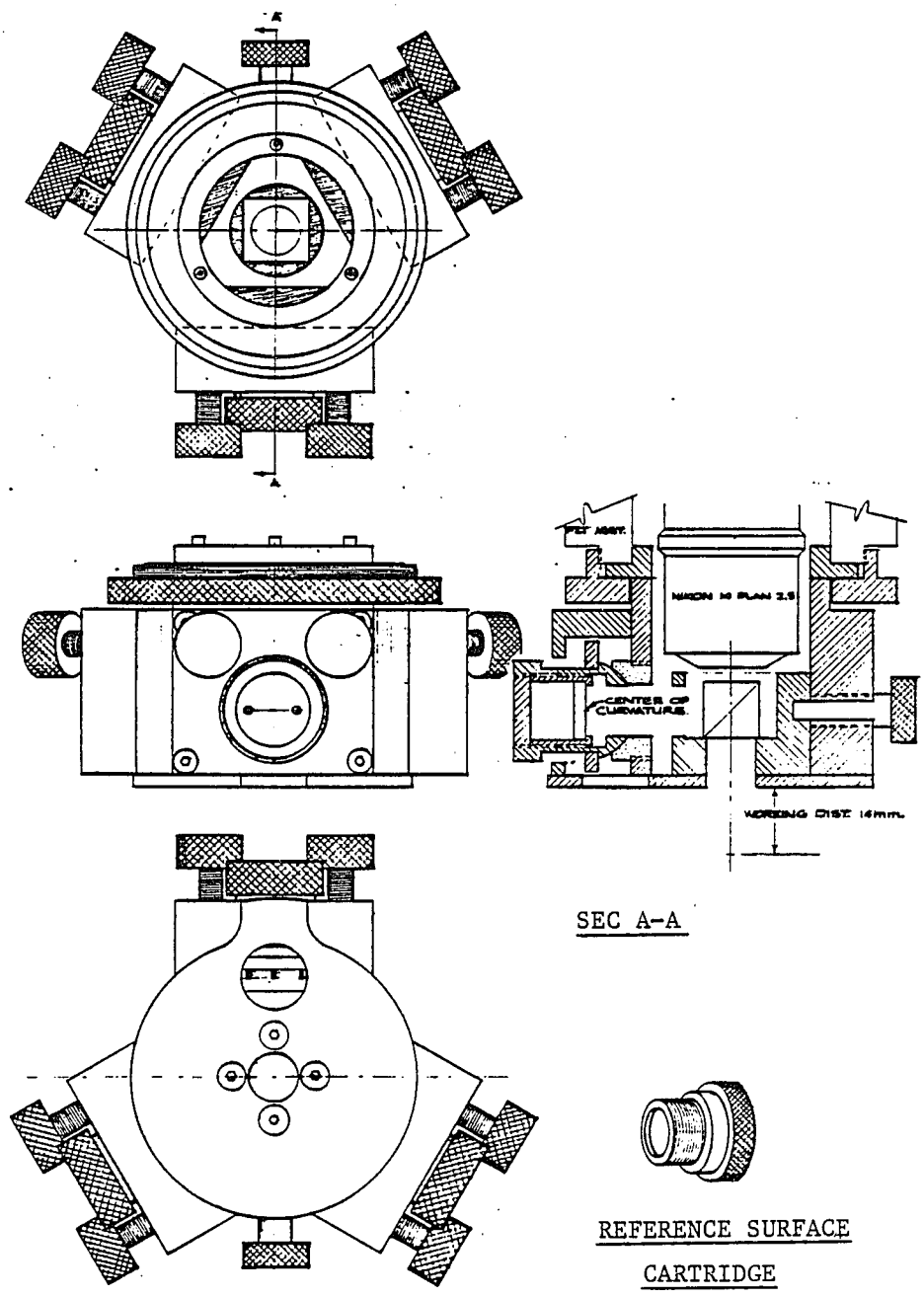

Fig. 18. Three mirror version.

requirements would seem to dictate a bearing of very high precision. If, however, this part is made with three lobes and wedged into place by a detent pin, the bearing needs to be only moderately precise. In this case the bearing locates the part only vertically and the semi-kinematic support of the lobes and the pin take care of the other degrees of freedom. A machined lip in the outer housing sandwiched between the three-lobed rotor and the index plate on the bottom provides an adequate bearing, and since the parts are anodized, wear is minimal.

It appears in the drawing that the beamsplitter rotor could be shortened to increase the system working distance by another 5 mm. or so. This would be a definite advantage in close quarters, but a rather complicated set of tradeoffs dictates the dimensions drawn. Shortening the rotor would either reduce the size of the reference mirror unacceptably or require another location for the spherical bearing. The given geometry, however, is simple and direct, both for tip-tilt adjustment and in support of longitudinal forces applied in changing reference cartridges; morever, good sensitivity for tip-tilt adjustments requires the longest arm possible for the adjusting screw to bear against. Fortunately, a square tip-tilt plate not only increases this lever arm as much as possible, but also prevents the female half of the spherical bearing from turning when the cartridge is changed.

The female half of the spherical bearing is threaded to allow placement of the center of rotation at the focus of the Nikon objective. Serrations on the rim of this half can be reached through a

hole in the indexing plate for adjustment after assembly. Once focus has been set, threadlocking liquid can be used to insure that the location of the center of rotation will not change.

A cartridge threads into the male half of the bearing, and is removable for replacement of the reference surface. Interchangeability of cartridges is maintained by virtue of the fact that the outer sleeve bottoms against the top of the male bearing; providing, therefore, that the top surface of the male half has a repeatable displacement from the center of curvature, cartridges can be preset to focus and will be interchangeable.

The remainder of the tip-tilt assembly consists of a rectangular housing, two 80 TPI ball-end adjusting screws, two opposing springs, a rectangular tip-tilt plate which is attached to the male bearing half with cyanoacrylate adhesive, and four mounting screws.

A flange and lock ring allow the assembly to be attached to the PZT firmly but with freedom of angular orientation. Knurling the lock ring allows sufficient leverage for a tight fit but prevents the use of excessive force on the relatively delicate PZT.

Version 2 (Figure 19), a single mirror version, is smaller and easier to manufacture than the triple version by virtue of its simplicity. Whether its simplicity ultimately is a virtue or a fault is properly the client's decision and will not be a concern of this study. This version has one special advantage, however: because of the extra space available on either side of the reference surface it is possible to attach geared motors to the housing for remote control of tip and

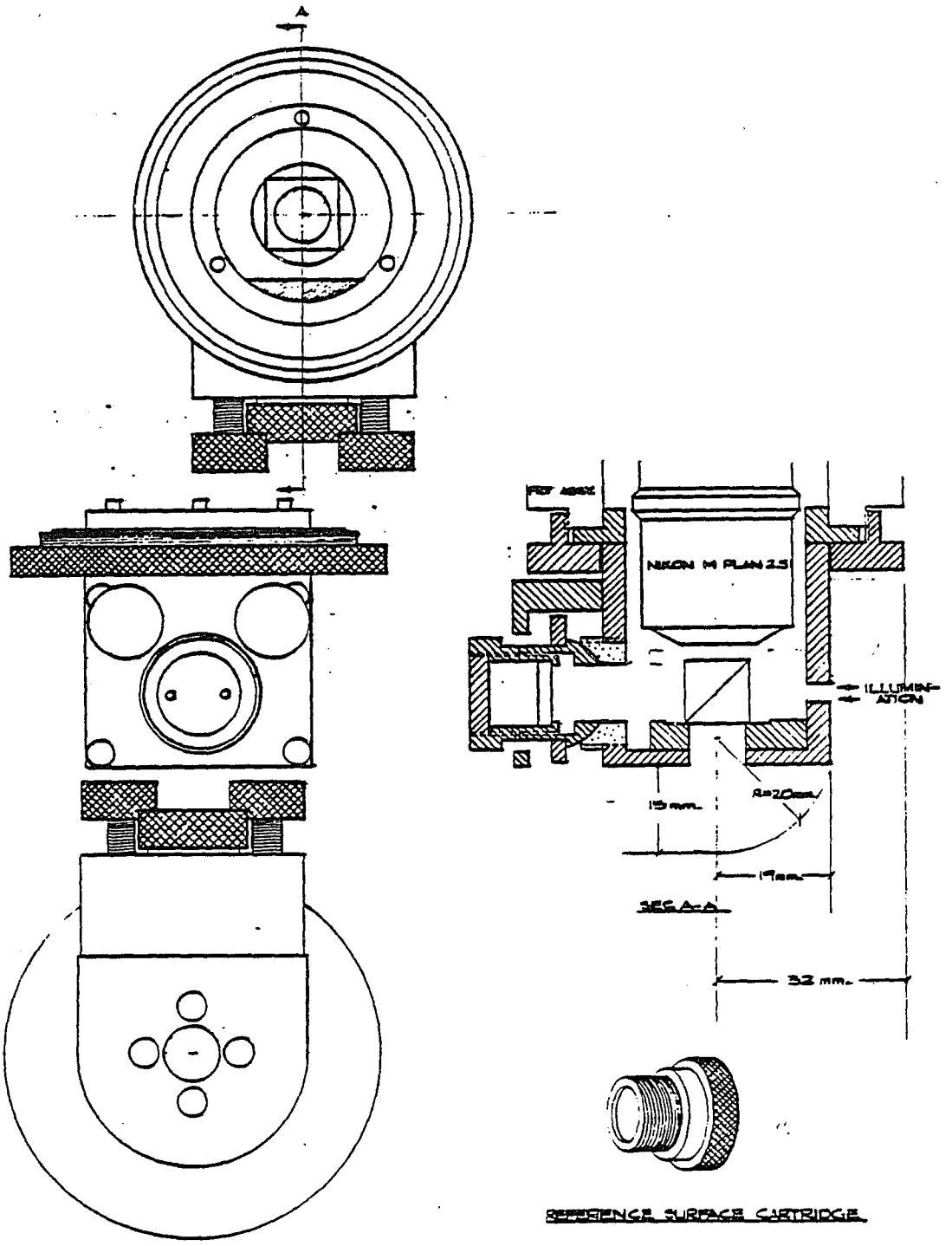

Fig. 19. Single mirror version.

tilt. This is especially useful for critical applications where the operator should not operate the controls manually.

The final version (Figure 20) takes advantage of the reversibility of the arms in the Michelson interferometer. This geometry makes it possible to look sideways at the test surface rather than along the axis of the microscope. Variation 1 has the greatest commonality of parts with the axial version and is therefore easiest to produce; its main drawback is the fact that the operator must have access to the end of the reference cylinder to adjust tip-tilt. Variation 2 solves this problem through motorization as in version no. 2 above. Variation 3 controls tip-tilt from above by constraining the reference mirror to move about a center of curvature located at the focus of the microscope objective. It uses the same cartridge as above.

Materials and Processes

The Michelson objective is designed to be built in a relatively simple machine shop by any competent machinist. It does not require any castings, forgings or extrusions, although these processes could improve production economy if the quantity was high enough. Required materials are brass, 6000 series aluminum alloy, molybdenum disulphide-filled nylon, and small amounts of readily available metals and hardware. The main machining operations required are turning, facing and boring (lathe and vertical milling machine). All drawing dimensions are in inches in recognition of widely available machines and tooling. Redesign in SI units would be straightforward. Where possible, commercially available parts have been specified to keep fabrication

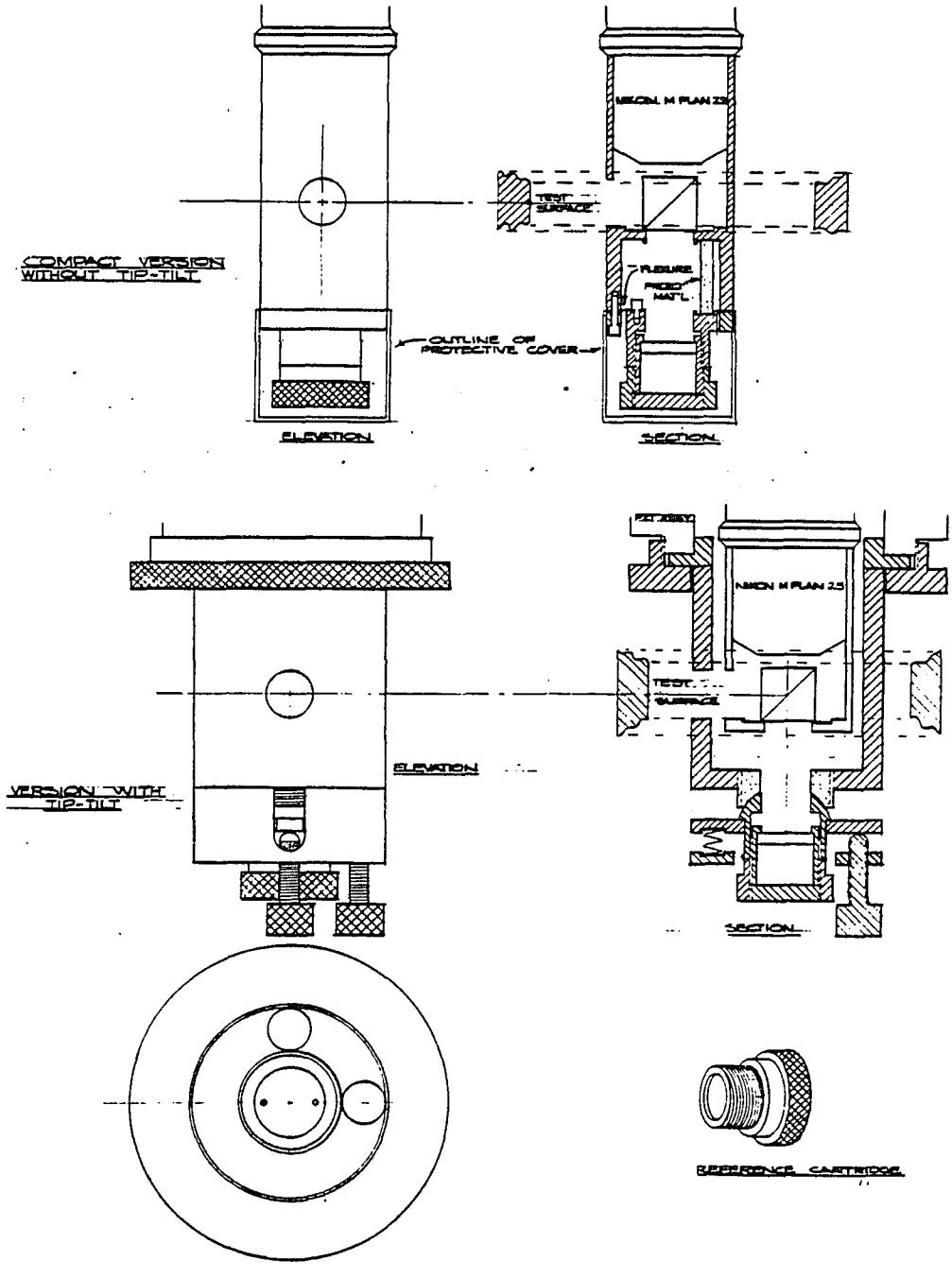

Fig. 20. Side-Looking Version.

costs to a minimum. Fabrication time for the prototype (machined parts only) was approximately 50 hours including making special fixtures, etc. In limited production this figure should drop to between thirty and forty hours.

Precise alignment of the beamsplitter requires special measures to ensure equal O.P.D. for all wavelengths. This problem was solved by buying high-quality beamsplitter halves separately and assembling them with precision jigs to achieve mechanical symmetry. High compliance epoxy optical adhesive was used to minimize mechanical deformation caused by shrinkage.

Super-polished reference mirrors were specially purchased to take advantage of the extremely high resolution of the basic instrument. They were mounted in the cells using a method suggested by Steve Lange of Wyko Optical to prevent deformation of the reference surface. This technique places room temperature vulcanizing (RTV) synthetic rubber through holes in the side of the cartridges. Any stress introduced by the RTV is therefore directed radially and least likely to affect the surface figure of the reference mirror.

Assembly and Alignment

Mechanical assembly is straightforward. Reference mirrors are installed in their respective cartridges at some trial position in the middle of their adjustment ranges. Using a test with some visible surface detail the female half of the spherical bearing is then screwed in or out until white light fringes are obtained. If these fringes move laterally with tip-tilt adjustment the reference surface and cartridge

are moved together until tilting the reference surface causes no lateral movement.

Attachment to the PZT is also simple and self-explanatory. The interferometer assembly can be oriented in any direction, but is most comfortable for right-handed users if the detent pin is 60 degrees to the right and one cartridge is centered facing the operator.

Testing

White light fringes were found within five minutes of initial assembly and profiles were taken a few minutes later. Tip-tilt screws are relatively sensitive but not unacceptably so. Profiles, with the exceptions noted below, were as expected.

Fringe visibility was only about 50% because of imbalance in the beamsplitter reflectance and transmittance figures. In the Mirau microscope illumination is provided by a Nikon Epi Illuminator; because the microscope is designed for use with reflecting surfaces Köhler illumination is directed through the imaging objective by a thin beamsplitter. This form of illumination has two drawbacks when used with the Michelson objective. The first results from the fact that the test beam transits the beamsplitter twice in transmission, while the reference surface passes twice in reflection. The ratio of irradiances at the surfaces therefore varies as the square of the ratio of reflectance to transmittance for the beamsplitter. The second drawback is a loss of 50% of the returning light to the illumination beamsplitter (as described in figure 24-a, page 61).

When the Epi Illuminator was replaced by a fiber optic illuminator operating through the cube beamsplitter the visibility increased to 90+%. Although the convenience of the Epi field stop as a focusing aid was lost, this feature could be added with a suitably designed illuminator.

The profiles in Figure 21 were taken using the Epi Illuminator. The first measurement uses high quality mirrors in both test and reference arms to check for beamsplitter aberrations. Successive profiles are uncorrected, corrected for tilt and corrected for curvature, respectively. A comatic aberration (odd symmetry) is clearly present.

A particularly useful feature of the profiler operating software is a feature which allows the storage of a given profile which can then be subtracted from all subsequent measurements. In Figure 22a, a reference profile was first measured and recorded using a superpolished reference surface. A second measurement was then taken in the same location on the test surface and the reference surface was subtracted (Figure 22b). A perfect measurement would be indicated by a flat horizontal line through the origin. The actual record shows both short and long wavelength noise. Because the long wavelength information is believed to represent mechanical movement in the profiler frame during the measurement, a local portion was selected in the third frame (Figure 22c) and the curvature and tilt correction algorithms available in the profiler software were applied. This final

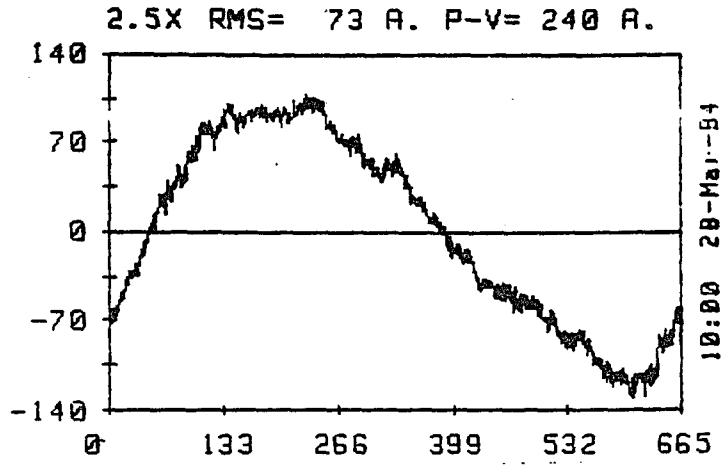

surface profile

(a)

distance on surface in microns

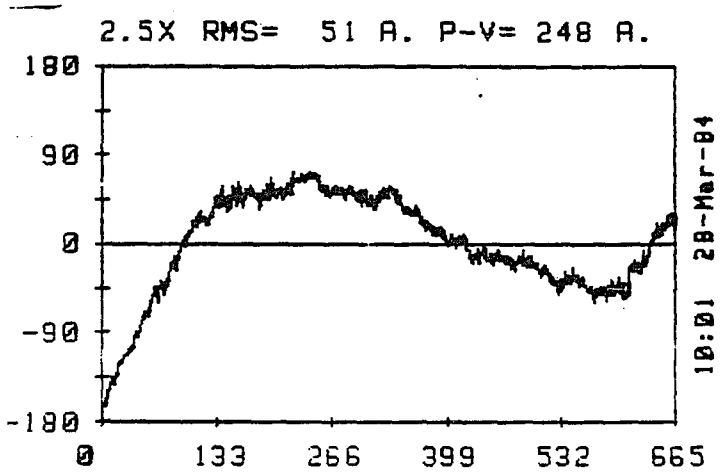

surface profile

(b)

distance on surface in microns

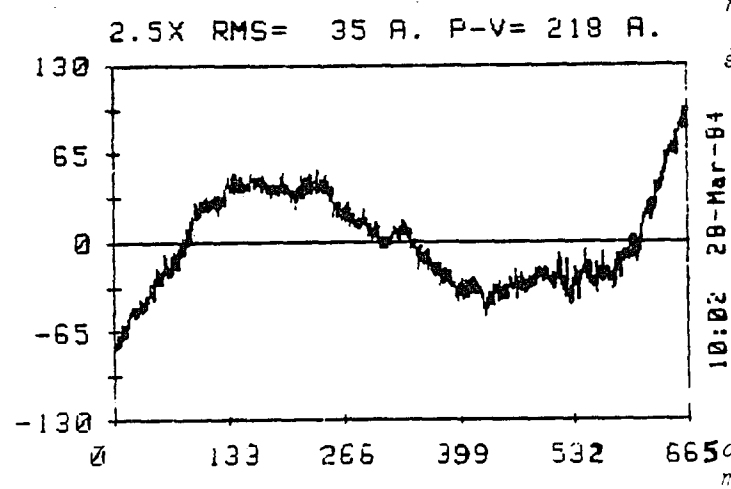

surface profile

(c)

distance on surface in microns

Fig. 21. Profile data showing beamsplitter induced profile error.

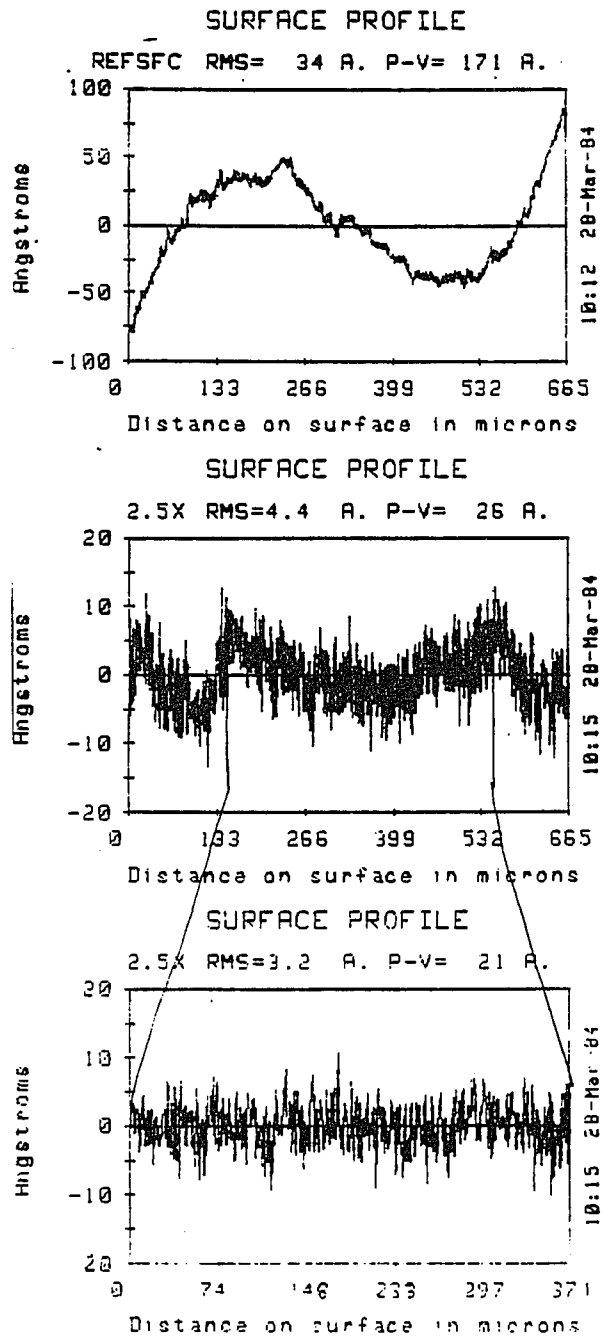

(a) Reference surface compared to surface-polished surface.

(b) Second measurement with 22-a subtracted.

(c) Portion of 22-b with tilt and curvature removed.

Fig. 22. Profile data showing reference subtraction technique.

trace is believed to represent a best-obtainable measurement of surface roughness with the present beamsplitter using the Epi illuminator.

Figure 23a is a check on the repeatability of measurements made with the 2.5x objective. These measurements were made by taking successive measurements at one location and subtracting them without subtracting the reference surface profile. This trace is comparable with that of Figure 22b. In Figure 23b an uncoated portion of the superpolished sample was measured and the reference surface was subtracted; and in Figure 23c a difference measurement on the uncoated surface, like that of Figure 23a, was taken. The general agreement of all of these measurements indicates that approximately five angstroms RMS surface roughness is the repeatability of this configuration.

To test the theory that the repeatability of the above measurements could be improved substantially by improving the visibility of the fringes a second set of measurements was taken, using fiber optic illumination. These measurements are summarized in Figure 24-a and 24-b. Here, a repeatability check was first taken and then the superpolished surface was measured using the reference subtraction technique. A substantial improvement in repeatibility is evident.

Further Comments on Beamsplitter Quality

Although it is possible to remove the beamsplitter effects on the measured sample using provisions of the profiler software, it would obviously be preferable to substitute a beamsplitter of better quality. The cube used in the present instrument was assembled by the author

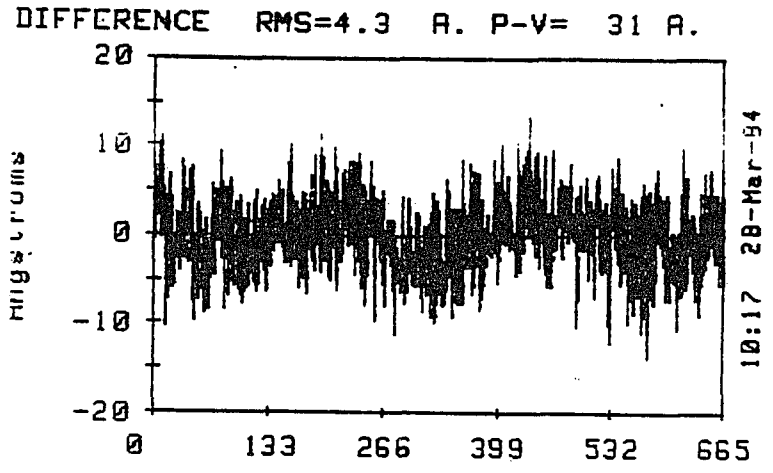

surface profile

(a)

distance on surface in microns

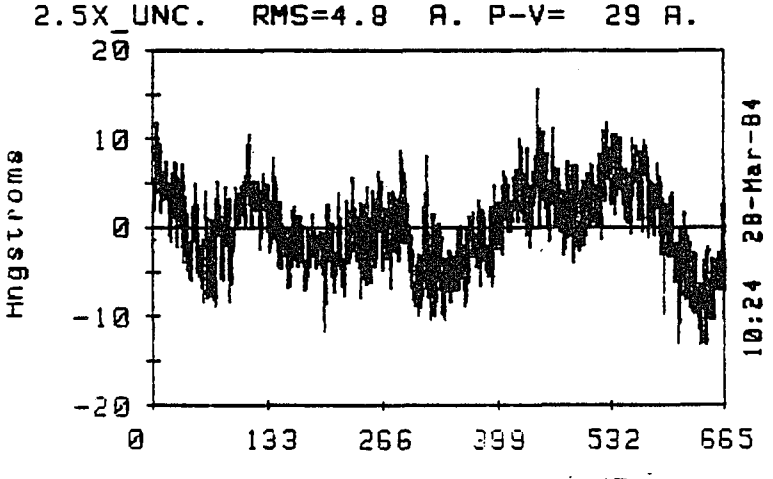

surface profile

(b)

distance on surface in microns

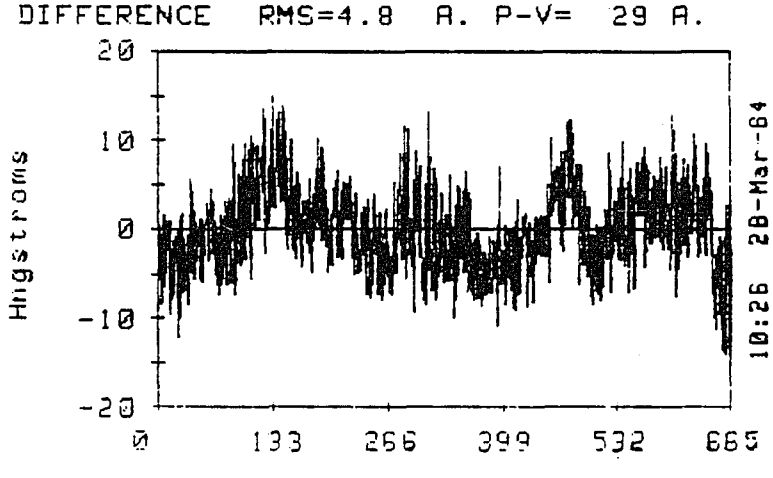

surface profile

(c)

distance on surface in microns.

Fig. 23. Repeatability checks of profile data.

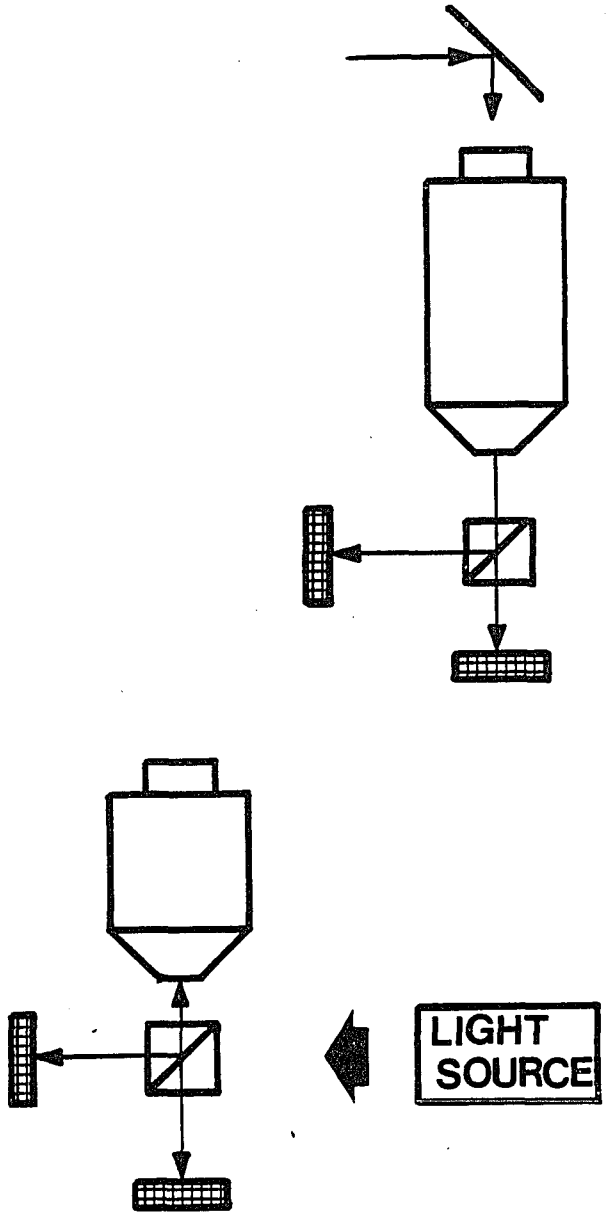

(a)

Fig. 24. Repeatability as affected by type of illumination.

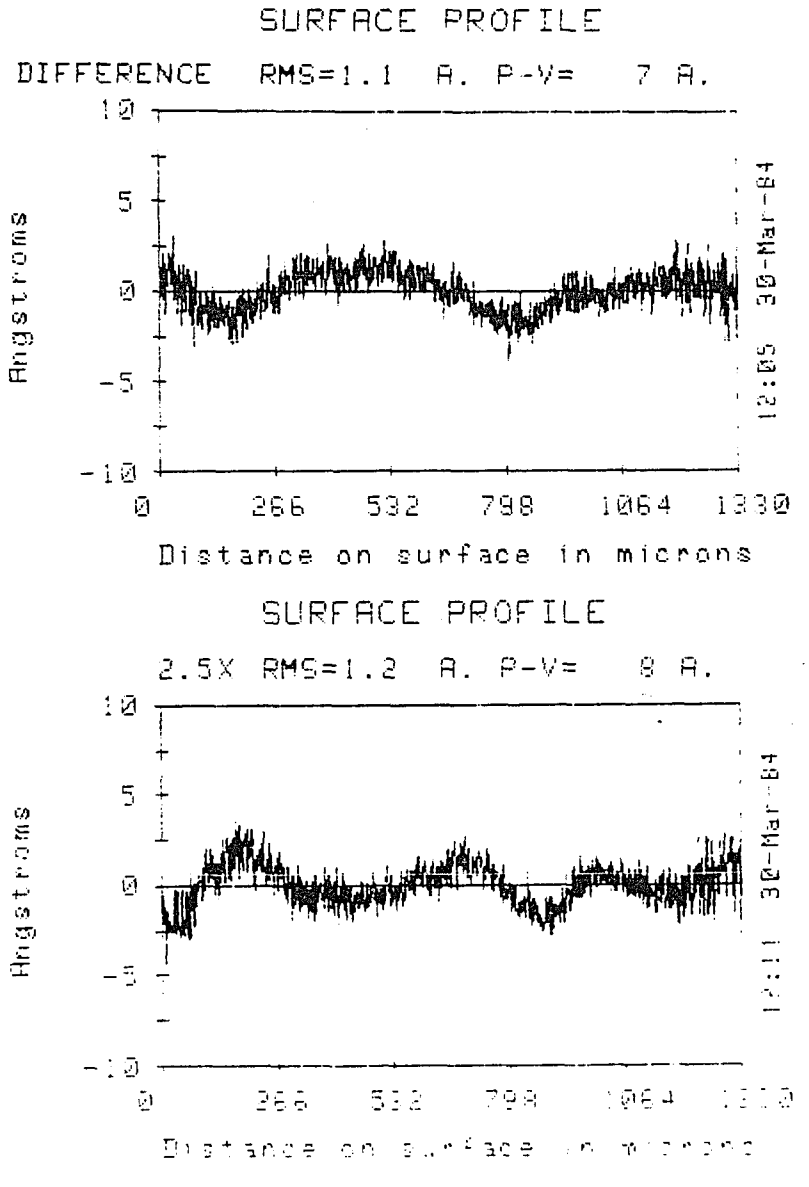

(b)

Fig. 24. Repeatability as affected by type of illumination.

(b) Super-polished surface (aluminized) with reference surface subtracted.

using low-shrinkage UV curing cement from halves supplied by a commercial source.

In order to understand the origins of the observed aberrations, the assembled cube and some unassembled halves were inspected using a Zygo interferometer. The specification on the beamsplitter hypotenuse and faces of 1/10 wave was met by all components. When checked in transmission, however, every piece showed substantial aberrations. Figure 25-a shows a typical interferogram of a beamsplitter half and the setup used to obtain the photograph (Figure 25-b). This test is admittedly quite sensitive because it is (1) taken in double pass; and (2) combines the effects of the faces, the hypotenuse and inhomogeneities in the BK7 glass. It is, however, quite representative of the conditions under which the cube is used.

Figure 26-a shows an interferogram obtained using the complete objective in Twyman-Green configuration, with the reference surface removed from the Zygo. About one fringe of coma is clearly evident in the photograph in Figure 26-b.

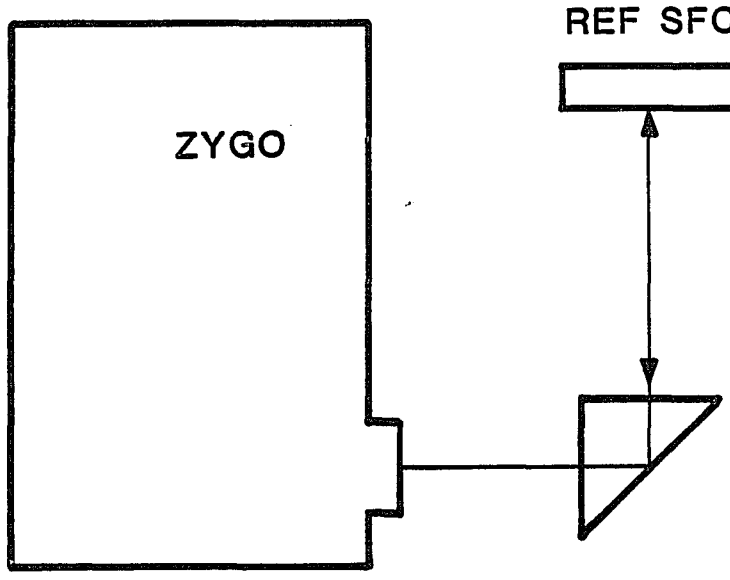

Fig. 25. Zygo interferometer test of cube half.

(a) Schematic drawing of setup used to test cube half.

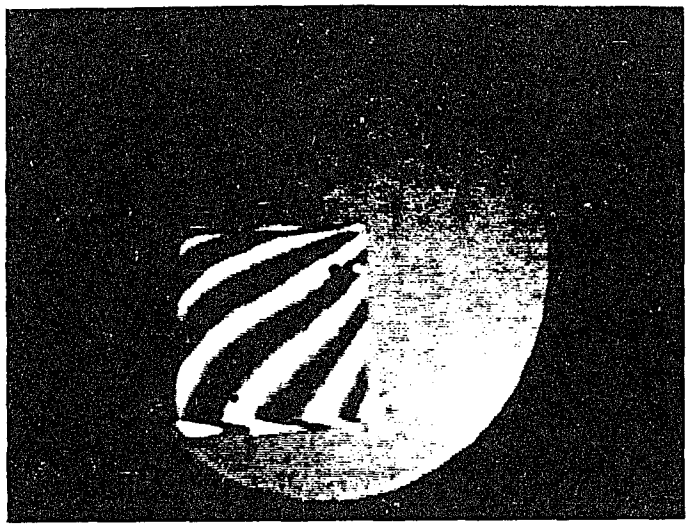

(b)

Fig. 25. (continued) Zygo interferometer test of cube half.

(b) Zygo interferogram of cube half.

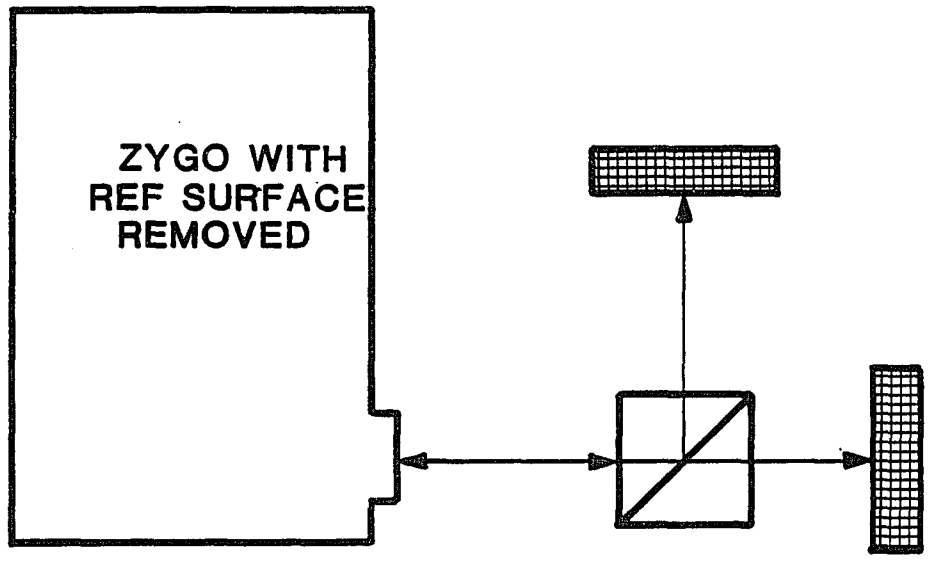

(a)

Fig. 26 . Zygo/Michelson test of completed cube.

(a) Schematic drawing of setup used to test completed cube.

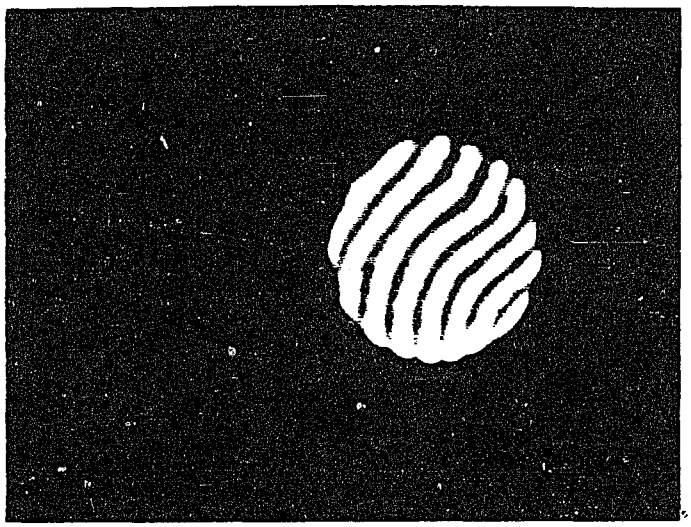

(b)

Fig. 26. (Continued) Zygo/Michelson test of completed cube.

(b) Zygo/Michelson interferogram of assembled cube.

CHAPTER 5

CONCLUSIONS

Once again the beamsplitter has been shown to be the critical component in the design. Inquiries to specialist prism manufacturers indicate that while special care is required to construct cube beamsplitters of the required quality, no unorthodox technology is involved. The investment of a reasonable amount of time, care and money should therefore bring about at least an order of magnitude improvement in performance. The decision of whether this investment is justified is, however, not strictly a technical one. Inquiries to various optical fabricators are continuing.

The system as designed met the goals established at the outset with the possible exception of beamsplitter quality. The process of refining the performance of this component is well understood and is continuing. As a commercial product, the 2.5x Michelson objective is not yet a reality. However, as a demonstration of feasibility, a test of sensitive parameters and a Master's Thesis project, it was a success.

Future development should clearly include the improvement of the beamsplitter, as well as exploration of the usefulness of the alternative versions as drawn in Figures 18-20. The use of the Michelson configuration opens up some interesting possibilities for the design of higher magnification systems with the beamsplitter either above or below the imaging objective. Advantages to this approach

include more efficient illumination, interchangeability of reference surfaces and greater working distance over the test surface.

REFERENCES

Hecht, E. and Zajac, A., Optics, (Addison-Wesley Publishing Co., Reading, 1974).

Koliopoulos, C. L. "Interferometric Optical Phase Measurement Optical Phase Measurement Techniques," Doctoral Dissertation, Optical Sciences Center, University of Arizona (1981).

Shack, Roland, Optical Sciences Center, University of Arizona, class notes and personal communications (1982-84).

Smith, W. Modern Optical Engineering, (McGraw-Hill, New York, 1966) p. 152.

Wyant, James C., Optical Sciences Center, University of Arizona, "Electronic Phase Measurement Techniques," class notes and personal communications, 1983-84).